

Function Approximation Technique-based Adaptive Force-Tracking Impedance Control for Unknown Environment

Norsinnira Zainul Azlan ^{a,1,*}, Hiroshi Yamaura ^{b,2}, Iswanto Suwarno ^{c,3}

^a Department of Mechatronics, Kulliyah of Engineering, International Islamic University Malaysia, Jalan Gombak, 53100 Kuala Lumpur, Malaysia

^b Department of Mechanical and Control Engineering, Tokyo Institute of Technology, Ookayama 2-12-1-I3-10 Meguro-ku, Tokyo, 158-8552, Japan

^c Department of Electrical Engineering, Universitas Muhammadiyah Yogyakarta, Kampus Terpadu UMY, Jl. Brawijaya, Kasihan, Bantul, Yogyakarta 55183, Indonesia

¹ sinnira@iium.edu.my; ² yamaura@mech.titech.ac.jp; ³ iswanto_te@umy.ac.id

* Corresponding Author

ARTICLE INFO

Article history

Received May 10, 2023

Revised December 16, 2024

Accepted January 10, 2024

Keywords

Adaptive Control;

Force Control;

Uncertain-Environment;

Time-Varying Uncertainties;

Robot Finger Control

ABSTRACT

An accurate force-tracking in various applications may not be achieved without a complete knowledge of the environment parameters in the force-tracking impedance control strategy. Adaptive control law is one of the methods that is capable of compensating parameter uncertainties. However, the direct application of this technique is only effective for time-invariant unknown parameters. This paper presents a Function Approximation Technique (FAT)-based adaptive impedance control to overcome uncertainties in the environment stiffness and location with consideration of the approximation error in the FAT representation. The target impedance for the control law have been derived for unknown time-varying environment location and constant or time-varying environment stiffness using Fourier Series. This allows the update law to be derived easily based on Lyapunov stability method. The update law is formulated based on the force error feedback. Simulation results in MATLAB environment have verified the effectiveness of the developed control strategy in exerting the desired amount of force on the environment in x-direction, while precisely follows the required trajectory along y-direction, despite the constant or time-varying uncertainties in the environment stiffness and location. The maximum force error for all unknown environment tested has been found to be less than 0.1 N. The test outcomes for various initial assumption of unknown stiffness between 20000N/m to 120000N/m have shown consistent and excellent force tracking. It is also evident from the simulation results that the proposed controller is effective in tracking time-varying desired force under the limited knowledge of the environment stiffness and location.

This is an open-access article under the [CC-BY-SA](https://creativecommons.org/licenses/by-sa/4.0/) license.



1. Introduction

Force control is crucial for various robot contact tasks [1]-[5] especially in industry, teleoperation, medical, hazardous material handling, and service robot applications. For example, in massaging, writing, welding and medical surgery, it is necessary to regulate the force exerted by the robot on the environment while it tracks a specified position trajectory in the orthogonal direction.

Two main control approaches adopted in compliant task include impedance control [1], [6]-[11] and hybrid position/force control [2], [12]-[15]. The objective of the impedance control strategy is to regulate the required dynamic relationship between the contact force and position of the robot's end-effector, referred to as 'target impedance'. Impedance control is inspired by the relationship between the voltage and current in electrical systems [1]. It provides a unified framework and less drastic change as the robot moves to contact space from free space compared to hybrid position/force control.

Impedance control with force-tracking capabilities has drawn the attention of numerous researchers [16]-[24]. The approach allows the specification of the desired force trajectory while maintaining the benefits of impedance control. By this, an accurate force-tracking can be achieved instead of compromising the force error and position error. However, the controller requires a complete knowledge of the environment stiffness and location beforehand, which may not be available in many practical cases [17], [18]. Environment stiffness can be defined as the measure of the amount of deflection that a load causes in a material, whereas 'environment location' [17]-[19], is also referred to as 'environment position' [19], [20]-[25], 'surface position' [25], 'environment geometry' [19] or 'geometry of the surface' [19] in the literature. The uncertainties in these parameters may be constant or time-varying (changes with time).

Force control with uncertain or unknown environment parameters is an active research area. Several techniques have been proposed in controlling the force exerted by the robot's end effector [17]-[39]. Yang et. al, [26] formulated an admittance adaptation method where the interaction torque is estimated by employing an observer. The robot's force at the interaction points is regulated by an admittance controller. In [27], the reference position trajectory is generated, and an adaptive control is implemented in reducing the inaccuracy due to the uncertainties in the environment parameters. Using impedance principal, a compliant control has been developed in [28] to compensate for unknown environment stiffness. The authors replace the required location in the impedance equation with the environment location. The inertia and damping coefficients are carefully selected so that the steady state error become zero. Cao et al. [29] combines the benefit of adaptive hybrid impedance (AHI) control and hybrid impedance control (HI). By this strategy, the error in the dynamic tracking phase become zero and the overshoots in the contact space can be eliminated. The update rate parameter is adapted online and any estimation on the modeling of the environment or robot is unnecessary.

In impedance control field for uncertain environment parameters, Wakamatsu et al. [30] developed an adaptive impedance controller utilizing Recursive Least Square (RLS) to estimate linear and nonlinear environmental stiffness. In [31], RLS is utilized to estimate the environment stiffness, damping and mass values. However, these methods are incapable of following the reference force since the environment location is not estimated. Li et al. [32] proposed a neural network-based adaptive impedance control to enhance human-robot collaboration tasks, but the approach is limited to zero-force tracking. Kim et al. [33] proposed adaptive Energy Bounding Algorithm (EBA) for controlling the robots in the industry to attain the required contact force with robust contact stability, even when there is a drastic change in the environmental stiffness. Nevertheless, the technique focuses on unknown changes in the environment stiffness only and the environment surface is set as flat.

Impedance control with force-tracking capability whilst able to compensate both unknown environment stiffness and location has been studied in [17]-[24], [34]-[36]. Impedance adaptation technique has been studied in [34] for optimal interaction of a robot with unknown environments by expressing the uncertain environment as linear systems with unknown dynamics. Seraji and Colbaugh [17] formulated two types of adaptive impedance control, namely 'direct adaptive scheme' and 'indirect adaptive' control. Komati et. al [35] extended the controller to microscale applications. Xie et al. [36] designed a two-loop adaptive impedance controller for robotic cell microinjection. The inner loop contains a target impedance and PI compensator, and the outer loop incorporates a reference position trajectory generator. However, the techniques in [17], [36] are limited to uncertain time-invariant environment parameters only. The controller in [17] also consists of undesirable contact force derivative, which is usually a noisy signal and may not provide meaningful information. As a

solution, the force derivative is approximated using the environment model, which in return, limits the application of the controller to unknown constant environment stiffness and location only. The method in [36] also focuses on the cases where the desired force is governed by ramp function only. This makes the approach to be unsuitable for the applications that require other time-varying reference forces. Many previous methods also focus on the time invariant uncertainties in which the controller can be derived directly from the adaptive control law. The solution for compensating systems with time varying uncertainties is more challenging as it is not straightforward and involves more steps.

An adaptive impedance control for overcoming uncertain time-varying environment stiffness and location has been developed by Jung and Hsia [18]. In the force-tracking impedance strategy, a two-phased control algorithm consisting of 'free space' and 'contact space' phases have been proposed. Nevertheless, the discontinuity of the stiffness gain parameter as it is switched from a high value to zero during the transition between these two phases may lead to instability in the event of unpredicted encounter with a stiff environment [38]. In addition, the force convergence analysis in the study is restricted for the cases where the error originated from the approximation of the environment shape, is a step function only. Lee and Buss [19], introduced an adaptation in the controller gain for a force-tracking impedance strategy. The method is suitable in dealing with unknown triangular shape, uncertain uneven environmental geometries, and sudden changes in the environment stiffness. However, the convergence of the error to zero for a nonconstant desired force is not guaranteed.

On the other hand, FAT is a method to represent general uncertainties with unknown variation bounds by orthonormal functions. The functions are comprised of the multiplication of finite time-invariant weight functions and time-varying basis functions. The update law for the constant weight functions can be obtained based on Lyapunov stability theory as in common adaptive control laws [21]-[25], [39]. This facilitates the estimation of the non-constant uncertain parameters and leads to the asymptotic convergence of the system error. The effectiveness of FAT-based controllers for various systems with uncertainties that vary with time have been reported in several studies [39]-[52]. Bai et al. formulated the controller for a class of nonholonomic systems using FAT method by separating the linear system and time-varying unknowns. By this, the stabilization issue of the nonholonomic system can be converted to adaptive control design and solved [40]. The work in [41] implemented the FAT method to design an immersion and invariance control, where the update law is obtained using the immersion and invariance technique. The researchers extend the FAT-based controller to drive multi-agent in avoiding dynamic obstacle, considering the restriction of the space. This makes the method to be more appealing for the real-life implementation [42]. The Coriolis and inertia matrices, and gravity vector of a rigid robot has been represented by Euler-Lagrange equation as the basis function in a FAT-based regressor free controller [43]. The real time experimental test conducted has verified the effectiveness of the developed controller [43]. FAT can also be implemented with a backstepping controller such in [44], where the FAT equations is used to describe uncertain external disturbances and system dynamics in an unknown passive torque simulator (PTS) system. FAT-based controller has also been developed to manipulate deformable object and avoid inappropriate handling of the object [45]. FAT is also utilized in deriving the adaptive controller to estimate the deformation Jacobian matrix (DJM) of the object. Phu et al. [46] simplifies the FAT method to decrease the adaptive system's order and to reduce the complexity in the calculations of previous FAT approach. The technique has been applied to a 4 DOF robot manipulator with flexible joints. FAT control has also demonstrated good results with less control effort in a prosthesis application using Hardware in Loop (HIL) setting, compared to the conventional computed torque and adaptive controllers [47]. The technique also has been implemented in an adaptive controller to control a robot manipulator where the measurement of the robot's velocity is not necessary and only the position feedback is needed in the control law [48]. Excellent performances can be observed under the control technique.

Most of previous studies focuses on solving for time invariant environment stiffness or/ and locations. The studies involving uncertain time-varying environment parameters are limited to a certain shapes or constant desired force. The solution for compensating systems with time varying

uncertainties is more challenging since it is not straightforward and involves further mathematical operations. From the literature also, it is evident that FAT can be applied for various systems with time-varying uncertainties, where the regressor matrix of the system is unnecessary. However, to the best of the authors' knowledge, the derivation a FAT-based control solution for a robot working in an unknown time-varying environment location and constant environment stiffness under various unknown environment conditions and desired forces, with the consideration of approximation error in the FAT representation can still be further explored.

This study presents an adaptive impedance control technique for robotic finger operating under a limited knowledge of the environment. The main contribution of this research is the formulation of an adaptive impedance controller with the force tracking capability to compensate for unknown time-varying environment location and constant environment stiffness, based on FAT method, with consideration of the approximation error in the FAT representation. The stability proof has been derived based on Lyapunov stability theory. Unlike other researches, the advantages of this method are:

- The derivative of the force feedback signal that is usually noisy is not required in this control law.
- No switching of the stiffness gain in the target impedance that may leads to instability, as the robot travels from noncontact to contact spaces is necessary.
- Time-varying desired forces can also be achieved under the proposed control technique. The method is not limited to constant reference force only.

Simulation tests has been conducted on time-varying environment location and constant stiffness, sinusoidally and non-continuous varying environment parameters, and inconstant desired forces. The effect of numerous values of initial guess on the environment stiffness has also been studied. The results under the proposed controller fulfills the control objective in providing an accurate force tracking in the force controllable direction, whilst following a predefined position trajectory in the position controllable direction. The rest of the paper is organized as follows. [Section 2](#) presents the FAT-based target impedance for unknown environment location and stiffness involving the derivation of the target impedance, update law and consideration on the approximation error with known and unknown upper bound. [Section 3](#) describes the impedance controller formula. The simulation results under various environment stiffness, location and desired forces are presented and discussed in [Section 4](#). Finally, conclusion is drawn in [Section 5](#).

2. FAT-based Target Impedance for Unknown Environment Location and Stiffness

The controller design starts with the derivation of the target impedance with the FAT representation and update law determination for the uncertain parameters based on Lyapunov stability theory. Then, the impedance controller is developed based on the derived target impedance. Under the target impedance formulation, the following cases are considered:

- FAT-based target impedance for unknown time-varying environment location and constant environment stiffness.
- FAT-based target impedance for unknown time-varying environment location and stiffness.
- Consideration on the approximation error with known upper bound for the above two cases.
- Consideration of the approximation error with unknown upper bound for the above two cases.

The controller design aims in formulating a control law to drive the robot's end effector to exert the required force on the environment in the force controllable direction, whilst tracking a predefined position trajectory in the position controllable direction in the contact space [\[20\]-\[23\]](#). The environment location and stiffness are not known accurately a priori. The end effector is desired to

follow a predefined position trajectory in the free space. Therefore, this study proposes a two-phase control algorithm for the force controllable direction, which are:

- (1) Free phase, where the robotic finger is not in contact with the environment yet; and
- (2) Contact phase, where the robotic finger is in contact with the environment.

The mathematical model of an n degree of freedom (DOF) robot can be described in the Cartesian space as.

$$M_x(X)\ddot{X} + C_x(X, \dot{X})\dot{X} + G_x(X) = F_{in} - F_e, \quad (1)$$

where $X \in \mathfrak{R}^{n \times 1}$, $\dot{X} \in \mathfrak{R}^{n \times 1}$ and $\ddot{X} \in \mathfrak{R}^{n \times 1}$ are the vector of the actual location, velocity and acceleration of the robot's end-effector in the operational space respectively, $M_x(X) \in \mathfrak{R}^{n \times n}$ is the symmetric positive definite inertia matrix, $C_x(X, \dot{X}) \in \mathfrak{R}^{n \times n}$ is the coriolis and centrifugal forces matrix, $F_{in} \in \mathfrak{R}^{n \times 1}$ is the vector of control input forces from the actuators, $G_x(X) \in \mathfrak{R}^{n \times 1}$ is the vector of gravitational forces, and $F_e \in \mathfrak{R}^{n \times 1}$ is the vector of forces exerted by the robot's end effector on the environment. The target impedance of an n DOF robot can be described as [20]-[23].

$$M_d\ddot{E} + B_d\dot{E} + K_dE = -K_fE_f \quad (2)$$

where $E \in \mathfrak{R}^{n \times 1}$ and $E_f \in \mathfrak{R}^{n \times 1}$ are the location vector and force error respectively, described by [20]-[23].

$$\begin{aligned} E &= X - X_d, \\ E_f &= F_e - F_d, \end{aligned} \quad (3)$$

$X_d \in \mathfrak{R}^{n \times 1}$ is the vector of the reference location, $F_d \in \mathfrak{R}^{n \times 1}$ is the vector of desired force, $\dot{E} \in \mathfrak{R}^{n \times 1}$ and $\ddot{E} \in \mathfrak{R}^{n \times 1}$ are the vectors of the velocity and acceleration errors respectively. $M_d \in \mathfrak{R}^{n \times n}$ is the diagonal symmetric positive definite desired inertia, $B_d \in \mathfrak{R}^{n \times n}$ is the diagonal symmetric positive definite desired damping factor, $K_d \in \mathfrak{R}^{n \times n}$ diagonal symmetric positive definite desired damping and $K_f \in \mathfrak{R}^{n \times n}$ is the force error factor matrices.

For simplicity, force is considered to be applied in one direction only. Let the elements of $M_d, K_f, B_d, K_d, F_d, F_e, X_d, X, \dot{E}, \ddot{E}, E$ and E_f be denoted as $m_d, k_f, b_d, k_d, f_d, f_e, x_d, x, \ddot{e}, \dot{e}, e$ and e_f respectively. Then, the target impedance (2) can be rewritten as [20]-[23].

$$m_d\ddot{e} + b_d\dot{e} + k_d e = -k_f e_f. \quad (4)$$

In the non-contact mode or free space, the robot is not in interaction with the environment. For this phase, $f_d = f_e = 0$. From (4), the impedance controller reduces to motion control and the control objective becomes location trajectory tracking. In this case, the reference location, x_d can be specified by the designer as the desired path for the robot, without considering the environment location and stiffness parameters. In the contact mode, the end effector is required to apply f_d on the environment. The reference trajectory, x_d that is needed to produce f_d precisely requires an exact information of the environment stiffness and location, where [17]-[18], [20]-[23].

$$x_d = x_e + (f_d/k_e) \quad (5)$$

x_e and k_e are the actual environment location and stiffness respectively. However, this information may not be known accurately beforehand in practice. In most cases, the environment location and stiffness may also not be constant, and the common adaptive controller could not be applied directly to provide a precise force-tracking.

2.1. FAT-based Target Impedance for Unknown Time-Varying Environment Location and Constant Environment Stiffness

The robot's end effector is required to apply the reference force, F_d on the environment while in contact mode. In this situation, the true values of the environment stiffness, K_e and location, X_e that are necessary to produce the desired force precisely, as governed in (5) may not be available a priori [18]. Defining the initial estimation of the environment stiffness, K'_e , initial estimation of the location, X'_e , inaccuracy in the estimation of the environment stiffness, δ_{K_e} and inaccuracy in the estimation of the environment location, δ_{X_e} , the FAT-based adaptive target impedance in compensating for uncertain environment location and constant environment stiffness with time-varying values can be proposed as.

$$\begin{aligned} X'_e &= X_e + \delta_{X_e}, \\ K'_e &= K_e + \delta_{K_e} \end{aligned} \quad (6)$$

$$B_d \dot{E}' + K_d E' + \theta_1 + \theta_2 + \theta_3 + \theta_4 + \theta_5 + \theta_6 = -K_f E_f \quad (7)$$

where $E' = X - X'_e$ and $\theta_1, \theta_2, \theta_3, \theta_4, \theta_5, \theta_6$ are the compensators introduced to overcome the uncertainties. Similarly, it is considered that the force is applied in one direction only for simplicity. Let $\dot{e}', e', x'_e, x_e, \dot{f}_d, \delta_{x_e}, \delta_{x_e}, \Omega_{(\cdot)}$ be the elements of $\dot{E}', E', X'_e, X_e, \dot{F}_d, \delta_{X_e}, \delta_{X_e}, \theta_{(\cdot)}$ respectively. Therefore, (6) and (7) can be rewritten as.

$$b_d \dot{e}' + k_d e' + \Omega_1 + \Omega_2 + \Omega_3 + \Omega_4 + \Omega_5 + \Omega_6 = -k_f e_f, \quad (8)$$

where $e' = x'_e - x$ and \dot{e}' is its time derivative. The compensators $\Omega_1, \Omega_2, \Omega_3, \Omega_4, \Omega_5$ and Ω_6 , can be expressed as.

$$\Omega_1 = -\frac{b_d \widehat{W}_1 Z_1}{k'_e}, \quad \Omega_2 = \frac{-k_d \widehat{W}_2 Z_2}{k'_e}, \quad \Omega_3 = \frac{b_d \widehat{W}_3 Z_3}{k'_e}, \quad (9)$$

$$\Omega_4 = (k_d \widehat{W}_4 Z_4) / k'_e, \quad \Omega_5 = (-b_d \dot{f}_d - k_d f_d) / k'_e, \quad \Omega_6 = -(k_f \widehat{W}_6 e_f) / k'_e$$

The values of k'_e and x'_e can be specified by the designer, $\widehat{W}_1 \in \mathfrak{R}^{1 \times \beta_1}, \widehat{W}_2 \in \mathfrak{R}^{1 \times \beta_2}, \widehat{W}_3 \in \mathfrak{R}^{1 \times \beta_3}, \widehat{W}_4 \in \mathfrak{R}^{1 \times \beta_4}$ and $\widehat{W}_6 \in \mathfrak{R}^{1 \times \beta_6}$ are the vectors of the estimated weighting function of the FAT expression and the true value of these estimations are constant; $Z_1 \in \mathfrak{R}^{\beta_1 \times 1}, Z_2 \in \mathfrak{R}^{\beta_2 \times 1}, Z_3 \in \mathfrak{R}^{\beta_3 \times 1}$ and $Z_4 \in \mathfrak{R}^{\beta_4 \times 1}$ are the vectors of the time-varying basis functions of the FAT representation, and $\beta_{(\cdot)}$ is the number of the basis functions employed.

Since the actual values of $\widehat{W}_{(\cdot)}$ are constants, Lyapunov stability theory can be used to obtain their update law as.

$$\begin{aligned} \dot{\widehat{W}}_1 &= -Q_1^{-1} b_d Z_1 e_f, \quad \dot{\widehat{W}}_2 = -Q_2^{-1} k_d Z_2 e_f, \quad \dot{\widehat{W}}_3 = Q_3^{-1} b_d Z_3 e_f, \\ \dot{\widehat{W}}_4 &= Q_4^{-1} k_d Z_4 e_f, \quad \dot{\widehat{W}}_6 = -Q_6^{-1} k_f e_f^2, \end{aligned} \quad (10)$$

where $Q_{(\cdot)}^{-1} \in \mathfrak{R}^{\beta_{(\cdot)} \times \beta_{(\cdot)}}$ are the diagonal positive definite symmetric matrices of the adaptation gain.

Theorem: Provided that the target impedance is achieved, the implementation of the proposed FAT-based target impedance (8) and adaptive update laws (10), on a robotic system operating under inexact knowledge of time-varying environment location and constant environment stiffness, leads to the asymptotic convergence of the force error to zero, $e_f \rightarrow 0$.

Proof: The force, f_e applied by the robotic finger on the environment, and its derivative \dot{f}_e can be obtained using the mathematical model of the environment as [17]-[18], [20]-[23].

$$\begin{aligned} f_e &= k_e(x - x_e), \\ \dot{f}_e &= k_e(\dot{x} - \dot{x}_e) \end{aligned} \quad (11)$$

Let f_{ee1} represents the inaccurate force applied to the environment because of the incomplete information of the constant environment stiffness and time-varying environment location. This variable be defined as.

$$f_{ee1} = (k_e + \delta_{ke})(x - (x_e + \delta_{xe})) \quad (12)$$

Since k_e and δ_{ke} in this case are constants, the derivative of (12), \dot{f}_{ee1} can be determined as

$$\dot{f}_{ee1} = (k_e + \delta_{ke})(\dot{x} - (\dot{x}_e + \dot{\delta}_{xe})) \quad (13)$$

Utilizing (12) and (13),

$$x = \frac{f_{ee1}}{(k_e + \delta_{ke})} + (x_e + \delta_{xe}), \quad \dot{x} = \frac{\dot{f}_{ee1}}{(k_e + \delta_{ke})} + (\dot{x}_e + \dot{\delta}_{xe}). \quad (14)$$

From (11) - (13), f_{ee1} and \dot{f}_{ee1} can also be rewritten as.

$$f_{ee1} = f_e + \delta_{ke}(x - (x_e + \delta_{xe})) - k_e\delta_{xe}, \quad (15)$$

$$\dot{f}_{ee1} = \dot{f}_e + \delta_{ke}(\dot{x} - (\dot{x}_e + \dot{\delta}_{xe})) - k_e\dot{\delta}_{xe}. \quad (16)$$

Substituting (14) - (16) into (8) and multiplying the resulting equation by k'_e , the modified target impedance becomes.

$$\begin{aligned} b_d\dot{e}_f + k_d e_f + b_d\delta_{ke}(\dot{x} - (\dot{x}_e + \dot{\delta}_{xe})) - b_d k_e \dot{\delta}_{xe} + k_d\delta_{ke}(x - (x_e + \delta_{xe})) \\ - k_d k_e \delta_{xe} + k_f(k_e + \delta_{ke})e_f - b_d\widehat{W}_1 Z_1 - k_d\widehat{W}_2 Z_2 + b_d\widehat{W}_3 Z_3 + k_d\widehat{W}_4 Z_4 \\ - k_f\widehat{W}_6 e_f = 0 \end{aligned} \quad (17)$$

The third to seventh term on the left-hand side of (17) are related to the inaccuracy in the estimation of the environment stiffness, δ_{ke} and location, δ_{xe} . These terms can be estimated using adaptive strategy by first expressing them using FAT representation, where.

$$\begin{aligned} \delta_{ke}(\dot{x} - (\dot{x}_e + \dot{\delta}_{xe})) &= W_1 Z_1 + \varepsilon_1, \\ \delta_{ke}(x - (x_e + \delta_{xe})) &= W_2 Z_2 + \varepsilon_2, \\ k_e \dot{\delta}_{xe} &= W_3 Z_3 + \varepsilon_3, \\ k_e \delta_{xe} &= W_4 Z_4 + \varepsilon_4, \\ \delta_{ke} &= W_6 + \varepsilon_6. \end{aligned} \quad (18)$$

And $W_{(\cdot)} \in \mathfrak{R}^{1 \times \beta_{(\cdot)}}$ are the constant true weighting vectors, and $\varepsilon_{(\cdot)}$ is the approximation error. At this stage, the approximation error, $\varepsilon_{(\cdot)}$ are regarded as zero since it is assumed that number of basis function utilized are a sufficient [20]-[23]. Then, the corresponding estimations of (18), as in the 8th to 12th term of (17) becomes.

$$\begin{aligned} \hat{\delta}_{ke}(\dot{x} - (\dot{x}_e + \dot{\delta}_{xe})) &= \widehat{W}_1 Z_1, \\ \hat{\delta}_{ke}(x - (x_e + \delta_{xe})) &= \widehat{W}_2 Z_2, \end{aligned} \quad (19)$$

$$\begin{aligned}\hat{k}_e \hat{\delta}_{xe} &= \hat{W}_3 Z_3, \\ \hat{k}_e \hat{\delta}_{xe} &= \hat{W}_4 Z_4, \\ \hat{\delta}_{ke} &= \hat{W}_6,\end{aligned}$$

where $\hat{W}_{(\cdot)} \in \mathfrak{R}^{1 \times \beta_{(\cdot)}}$ are the estimation of $W_{(\cdot)}$ [20]-[23].

In (18) and (19), it can be observed that, FAT can be used to estimate time-varying expressions, including the ones which are the functions of x and \dot{x} . Since the expressions are represented as the multiplication of the vectors of the constant weighting and time-varying basis functions, Lyapunov stability theory can be used to easily determine the adaptive update law. On the contrary, this cannot be done by adopting the standard adaptive scheme directly. Substituting (18) into (17), and defining the estimation error as $\tilde{W}_{(\cdot)} = W_{(\cdot)} - \hat{W}_{(\cdot)}$, the modified target impedance becomes.

$$b_d \dot{e}_f + (k_d + k_e k_f) e_f + b_d \tilde{W}_1 Z_1 + k_d \tilde{W}_2 Z_2 - b_d \tilde{W}_3 Z_3 - k_d \tilde{W}_4 Z_4 + k_f \tilde{W}_6 e_f = 0 \quad (20)$$

The Lyapunov-like function candidate can be selected as.

$$V = \frac{1}{2} e_f^T b_d e_f + \frac{1}{2} \tilde{W}_1^T Q_1 \tilde{W}_1 + \frac{1}{2} \tilde{W}_2^T Q_2 \tilde{W}_2 + \frac{1}{2} \tilde{W}_3^T Q_3 \tilde{W}_3 + \frac{1}{2} \tilde{W}_4^T Q_4 \tilde{W}_4 + \frac{1}{2} \tilde{W}_6^T Q_6 \tilde{W}_6 \quad (21)$$

Differentiating (21) with respect to time yields.

$$\dot{V} = e_f^T b_d \dot{e}_f - \tilde{W}_1^T Q_1 \dot{\tilde{W}}_1 - \tilde{W}_2^T Q_2 \dot{\tilde{W}}_2 - \tilde{W}_3^T Q_3 \dot{\tilde{W}}_3 - \tilde{W}_4^T Q_4 \dot{\tilde{W}}_4 - \tilde{W}_6^T Q_6 \dot{\tilde{W}}_6. \quad (22)$$

Substituting $b_d \dot{e}_f$ from (20) into (22) gives.

$$\begin{aligned}\dot{V} &= -e_f^T (k_d + k_e k_f) e_f + \tilde{W}_1^T [-b_d Z_1 e_f - Q_1 \dot{\tilde{W}}_1] + \tilde{W}_2^T [-k_d Z_2 e_f - Q_2 \dot{\tilde{W}}_2] \\ &\quad + \tilde{W}_3^T [b_d Z_3 e_f - Q_3 \dot{\tilde{W}}_3] + \tilde{W}_4^T [k_d Z_4 e_f - Q_4 \dot{\tilde{W}}_4] + \tilde{W}_6^T [-k_f e_f^2 - Q_6 \dot{\tilde{W}}_6]\end{aligned} \quad (23)$$

Substituting the adaptive update laws (10) into (24), \dot{V} can finally becomes.

$$\dot{V} = -e_f^T (k_d + k_e k_f) e_f \quad (24)$$

The second time derivative of (23) can be obtained as.

$$\ddot{V} = -2e_f^T (k_d + k_e k_f) \dot{e}_f \quad (25)$$

From (21) and (24), since V is positive definite and \dot{V} is negative semi-definite, it can be concluded that the force error, e_f and estimation errors $\tilde{W}_{(\cdot)}$ are bounded. From (20) and (25) it can be deduced that \ddot{V} is also bounded. Therefore, using Barbalat's lemma, $\lim_{t \rightarrow \infty} \dot{V} = 0$, which implies that $\lim_{t \rightarrow \infty} e_f = 0$ and $\lim_{t \rightarrow \infty} \dot{e}_f = \dot{f}_d$.

Remark 1: Note that in (19), $\hat{\delta}_{ke}$ is represented by \hat{W}_6 , without being multiplied by a basis function since the unknown environment stiffness is constant in this case.

2.2. Consideration on the Approximation Error with Known Upper Bound for Unknown Time-Varying Environment Location and Constant Environment Stiffness

The controller development in Section 2.1 assumes that there is enough number of basis function in FAT representation and thus, the approximation error in (18) is regarded to be zero [20]-[23]. However, in the event where there is insufficient number of basis functions, the approximation error in the Fourier Series in (18) need to be taken into account. Otherwise, the proposed target impedance (8) may not guarantee the convergence of the force error to zero. Assuming the complete information

of the upper bound for the approximation error is available, then target impedance (8) can be adjusted by inserting a new compensator, $\Omega_{robust3}$,

$$b_d \dot{e}' + k_d e' + \Omega_1 + \Omega_2 + \Omega_3 + \Omega_4 + \Omega_5 + \Omega_6 + \Omega_{robust3} = -k_f e_f \quad (26)$$

Where

$$\Omega_{robust3} = \frac{\delta_{robust3} \text{sgn}(e_f)}{k'_e} \quad (27)$$

And $\delta_{robust3}$ is a positive constant such that $\|\varepsilon_{total3}\| \leq \delta_{robust3}$, and $\varepsilon_{total3} = b_d \varepsilon_3 - b_d \varepsilon_1 + k_d \varepsilon_4 - k_d \varepsilon_2$. Substituting (14)-(16) into (26), utilizing (18) and multiplying the equation with k'_e yields.

$$\begin{aligned} & b_d \dot{e}_f + (k_d + k_e) e_f + b_d \tilde{W}_1 Z_1 + k_d \tilde{W}_2 Z_2 - b_d \tilde{W}_3 Z_3 \\ & - k_d \tilde{W}_4 Z_4 + k_f \tilde{W}_6 e_f + b_d \varepsilon_1 + k_d \varepsilon_2 - b_d \varepsilon_3 - k_d \varepsilon_4 + k'_e \Omega_{robust3} = 0 \end{aligned} \quad (28)$$

In comparison to (20), (28) contains additional terms which are due to the approximation errors $\varepsilon_1, \varepsilon_2, \varepsilon_3$ and ε_4 , and the compensator, $\Omega_{robust3}$. Choosing the same Lyapunov-like function candidate as (21) and substituting $b_d \dot{e}_f$ from (28) and update law (10) into its derivative, \dot{V} can be rewritten as.

$$\dot{V} = -e_f (k_d + k_e k_f) e_f + e_f \varepsilon_{total3} - k'_e e_f \Omega_{robust3} \quad (29)$$

And

$$\dot{V} \leq -e_f (k_d + k_e k_f) e_f + \|e_f\| \delta_{robust3} - k'_e e_f \Omega_{robust3} \quad (30)$$

Substituting (27) into (30) gives

$$\dot{V} \leq -e_f (k_d + k_e k_f) e_f \leq 0 \quad (31)$$

which is similar to the result in (24). Similarly, using Barbalat's lemma as in Section 2.1, the convergence of the force error to zero can be proven. The $\text{sgn}(e_f)$ function in (27) can be replaced with the continuous function, $\frac{e_f}{\delta_{ef} + |e_f|}$ to avoid chattering effect in the tracking outcomes.

2.3. Consideration of the Approximation Error with Unknown Upper Bound for Unknown Time-Varying Environment Location and Constant Environment Stiffness

If an insufficient number of basis functions is utilized, the approximation error in the Fourier series (18) will be significant. Suppose that the upper bound of the approximation error is unknown, the stability of the system with target impedance (8) can be guaranteed by modifying the update laws by introducing σ -modification terms where.

$$\begin{aligned} \hat{W}_1 &= -Q_1^{-1}(b_d Z_1 e_f + \sigma_1 \hat{W}_1), \\ \hat{W}_2 &= -Q_2^{-1}(k_d Z_2 e_f + \sigma_2 \hat{W}_2), \\ \hat{W}_3 &= Q_3^{-1}(b_d Z_3 e_f - \sigma_3 \hat{W}_3), \\ \hat{W}_4 &= Q_4^{-1}(k_d Z_4 e_f - \sigma_4 \hat{W}_4), \\ \hat{W}_6 &= -Q_6^{-1}(k_f e_f^2 + \sigma_k \hat{W}_k). \end{aligned} \quad (32)$$

and $\sigma_{(\cdot)}$ are positive constants. The detailed explanation on the stability analysis with the σ -modification terms for unknown upper bound of the approximation error, where the system errors $e_f, \tilde{W}_k, \tilde{W}_1, \tilde{W}_2, \tilde{W}_3$ and \tilde{W}_4 are uniformly ultimately bounded can be found in [23].

2.4. FAT-based Target Impedance for Unknown Time-Varying Environment Location and Stiffness

The target impedance in (7) is extended to deal with both uncertain time-varying environment location and stiffness conditions. Therefore, during contact phase, the target impedance in the force controllable direction is proposed as [20]-[23].

$$B_d \dot{E}' + K_d E' + \Theta_1 + \Theta_2 + \Theta_3 + \Theta_4 + \Theta_5 + \Theta_{6v} + \Theta_{7v} = -K_f E_f \quad (33)$$

Similarly, force is exerted in one direction only. Therefore, (33) can be written as [20]-[23].

$$b_d \dot{e}' + k_d e' + \Omega_1 + \Omega_2 + \Omega_3 + \Omega_4 + \Omega_5 + \Omega_{6v} + \Omega_{7v} = -k_f e_f. \quad (34)$$

The compensators $\Omega_1, \Omega_2, \Omega_3, \Omega_4, \Omega_5$ are similar to the ones in (8). Ω_{6v} is modified from Ω_6 and Ω_{7v} is added to overcome the nonconstant uncertainties in the environment stiffness. These compensators can be expressed as [21].

$$\Omega_{6v} = -(k_f \hat{W}_{6v} Z_{6v} e_f) / k'_e, \quad \Omega_{7v} = b_d \hat{W}_{7v} Z_{7v} / k'_e, \quad (35)$$

where $\hat{W}_{6v} \in \mathfrak{R}^{1 \times \beta_{6v}}$ and $\hat{W}_{7v} \in \mathfrak{R}^{1 \times \beta_{7v}}$ are the estimated constant vectors of weighting function, and $Z_{6v} \in \mathfrak{R}^{\beta_{6v} \times 1}$ and $Z_{7v} \in \mathfrak{R}^{\beta_{7v} \times 1}$ are the time-varying vectors of basis function of the FAT representation, which are introduced to overcome the uncertain time-varying environment stiffness. By the application of Lyapunov stability theory, the update laws for the adaptation can be obtained as.

$$\begin{aligned} \hat{W}_{6v} &= -Q_{6v}^{-1} k_f Z_{6v} e_f^2, \\ \hat{W}_{7v} &= Q_{7v}^{-1} b_d Z_{7v} e_f. \end{aligned} \quad (36)$$

Theorem: Given that the target impedance is attained, with the FAT adaptive target impedance (34), update laws (36) and the first 4 update laws in (10), the force error asymptotically converges to zero, $e_f \rightarrow 0$ and the force exerted by the robot's end effector converges the desired value, $f_e \rightarrow f_d$ and as $t \rightarrow \infty$, despite the time-varying uncertainties in the environment parameters.

Proof: From f_e in (11), the derivative of the force applied by the robotic finger, considering the time-varying uncertainty in the environment stiffness. \dot{f}_{ev} can be written as [21].

$$\dot{f}_{ev} = k_e (\dot{x} - \dot{x}_e) + \dot{k}_e (x - x_e). \quad (37)$$

From (12), the derivative of the inaccurate force due to both uncertain time-varying environment stiffness and location, denoted as \dot{f}_{ee1v} can be derived as [21].

$$\dot{f}_{ee1v} = (k_e + \delta_{ke}) (\dot{x} - (\dot{x}_e + \delta_{xe})) + (\dot{k}_e + \delta_{ke}) (x - (x_e + \delta_{xe})). \quad (38)$$

Substituting x and \dot{x} from (14) into the FAT-based adaptive target impedance in (34) results in [21].

$$b_d \left(\frac{\dot{f}_{ee1v}}{k'_e} - \frac{(k_e + \delta_{ke})(x - (x_e + \delta_{xe}))}{k'_e} \right) - \frac{b_d \dot{f}_d - k_d f_d}{k'_e} + \frac{-b_d \hat{W}_1 Z_1 - k_d \hat{W}_2 Z_2}{k'_e} + \frac{b_d \hat{W}_{7v} Z_{7v}}{k'_e} + k_d \frac{f_{ee1}}{k'_e} + \frac{b_d \hat{W}_3 Z_3 + k_d \hat{W}_4 Z_4}{k'_e} - \frac{k_f \hat{W}_{6v} Z_{6v} e_f}{k'_e} = -k_f e_f. \quad (39)$$

and then utilizing (15) and (38), the target impedance in (39) can be further expanded as [21].

$$b_d \frac{\dot{e}_f}{k'_e} + k_d \frac{e_f}{k'_e} + \frac{b_d \delta_{ke}(\dot{x} - (\dot{x}_e + \delta_{xe}))}{k'_e} - \frac{k_f \widehat{W}_{6v} Z_{6v} e_f}{k'_e} + \frac{k_d \delta_{ke}(x - (x_e + \delta_{xe}))}{k'_e} + \frac{-b_d k_e \delta_{xe} - k_d k_e \delta_{xe}}{k'_e} + \frac{-b_d k_e (x - x_e)}{k'_e} + \frac{-b_d \widehat{W}_1 Z_1 - k_d \widehat{W}_2 Z_2}{k'_e} + \frac{b_d \widehat{W}_3 Z_3 + k_d \widehat{W}_4 Z_4}{k'_e} + \frac{b_d \widehat{W}_{7v} Z_{7v}}{k'_e} = -k_f e_f \quad (40)$$

Using FAT, the following functions can be expressed as [21].

$$\delta_{ke} = W_{6v} Z_{6v} + \varepsilon_{6v}, \quad \dot{k}_e(x - x_e) = W_{7v} Z_{7v} + \varepsilon_{7v}, \quad (41)$$

and their respective estimations can be written as [21].

$$\hat{\delta}_{ke} = \widehat{W}_{6v} Z_{6v}, \quad \hat{k}_e(x - \hat{x}_e) = \widehat{W}_{7v} Z_{7v}. \quad (42)$$

In (41), a sufficient number of basis functions is assumed that used in the controller and therefore $\varepsilon = 0$. Substituting $W_1, Z_1, W_2, Z_2, W_3, Z_3, W_4, Z_4$ from (18), and the FAT representations in (41)-(42) into (40), and multiplying k'_e with the resulting equation gives [21].

$$b_d \dot{e}_f = -(k_d + k_f k_e) e_f - b_d \widehat{W}_1 Z_1 + b_d \widehat{W}_3 Z_3 - k_d \widehat{W}_2 Z_2 + k_d \widehat{W}_4 Z_4 + b_d \widehat{W}_{7v} Z_{7v} - k_f \widehat{W}_{6v} Z_{6v} e_f. \quad (43)$$

The Lyapunov-like function candidate is chosen as [21].

$$V = \frac{1}{2} e_f^T b_d e_f + \frac{1}{2} \widetilde{W}_1^T Q_1 \widetilde{W}_1 + \frac{1}{2} \widetilde{W}_2^T Q_2 \widetilde{W}_2 + \frac{1}{2} \widetilde{W}_3^T Q_3 \widetilde{W}_3 + \frac{1}{2} \widetilde{W}_4^T Q_4 \widetilde{W}_4 + \frac{1}{2} \widetilde{W}_{6v}^T Q_{6v} \widetilde{W}_{6v} + \frac{1}{2} \widetilde{W}_{7v}^T Q_{7v} \widetilde{W}_{7v}. \quad (44)$$

Substituting $b_d \dot{e}_f$ from (43), the update laws for $\dot{\widehat{W}}_1, \dot{\widehat{W}}_2, \dot{\widehat{W}}_3, \dot{\widehat{W}}_4$ from (10) and the adaptation law for $\dot{\widehat{W}}_{6v}, \dot{\widehat{W}}_{7v}$ from (36) into the derivative of (44), \dot{V} can be finally reduced to [21].

$$\dot{V} = -e_f^T (k_d + k_e k_f) e_f. \quad (45)$$

Since $V > 0$ and $\dot{V} \leq 0$ as can be seen in (44) and (45) respectively, the estimation errors $\widetilde{W}_{(i)}$ and force error, e_f are the bounded. To evaluate the convergence of e_f , \dot{V} can be differentiated and \ddot{V} is also bounded, while \dot{V} is uniformly continuous. Therefore, utilizing Barbalat's lemma, it can be deduced that $\lim_{t \rightarrow \infty} \dot{V} = 0$. From (45), this implies that $\lim_{t \rightarrow \infty} e_f = 0$ and $\lim_{t \rightarrow \infty} \dot{e}_f = \dot{f}_d$ [21].

Remark 2: In comparison to the FAT representation of δ_{ke} by \widehat{W}_6 in (19), the $\hat{\delta}_{ke}$ for uncertain time-varying environment stiffness in (42) is represented by the multiplication of the time-varying basis function and constant weighting function, i.e. $\widehat{W}_{6v} Z_{6v}$. This is because $\hat{\delta}_{ke}$ in (42) is an uncertain time-varying environment stiffness.

Remark 3: It should be noted that all the target impedances and update laws proposed in (7)-(10), (33)-(36) do not require the noisy force feedback derivative signal, \dot{f}_e . This property is useful in the practical implementation of the controller.

2.5. Consideration on the Approximation Error with Known Upper Bound for Unknown Time-Varying Environment Location and Stiffness

Suppose that an insufficient number of basis function is utilized and therefore, the approximation error in the Fourier Series in (18) and (41) cannot be ignored, the proposed target impedance (34) is unable to guarantee the convergence of the force error to zero. This problem can be solved by incorporating a new compensator, $\Omega_{robust4}$ in target impedance (34) if the information of the upper bound of the approximation error is available, giving.

$$b_d(\dot{x}'_e - \dot{x}) + k_d(x'_e - x) + \Omega_1 + \Omega_2 + \Omega_3 + \Omega_4 + \Omega_5 + \Omega_{6v} + \Omega_{7v} + \Omega_{robust4} = -k_f e_f \quad (46)$$

where

$$\Omega_{robust4} = \frac{\delta_{robust4} \text{sgn}(e_f)}{k'_e} \quad (47)$$

$\delta_{robust4}$ is a positive constant such that $\|\varepsilon_{total4}\| \leq \delta_{robust4}$, and $\varepsilon_{total4} = b_d \varepsilon_3 - b_d \varepsilon_1 + k_d \varepsilon_4 - k_d \varepsilon_2 + b_d \varepsilon_{7v} - k_f \varepsilon_{6v} e_f$.

The stability proof can be found by rearranging and substituting (37)-(38) into (46) and multiplying the equation with k'_e yields.

$$\begin{aligned} & b_d \dot{e}_f + (k_d + k_f k_e) e_f + b_d \tilde{W}_1 Z_1 + k_d \tilde{W}_2 Z_2 - b_d \tilde{W}_3 Z_3 - k_d \tilde{W}_4 Z_4 - b_d \tilde{W}_{7v} Z_{7v} \\ & + k_f \tilde{W}_{6v} Z_{6v} e_f + b_d \varepsilon_1 + k_d \varepsilon_2 - b_d \varepsilon_3 - k_d \varepsilon_4 - b_d \varepsilon_{7v} + k_f \varepsilon_{6v} e_f + k'_e \Omega_{robust4} = 0 \end{aligned} \quad (48)$$

Choosing the same Lyapunov-like function candidate as (44) and substituting $b_d \dot{e}_f$ from (48) and update laws (10), (36) into its derivative, \dot{V} can be rewritten as.

$$\dot{V} = -e_f (k_d + k_e k_f) e_f + e_f \varepsilon_{total4} - k'_e e_f \Omega_{robust4} \quad (49)$$

And

$$\dot{V} \leq -e_f (k_d + k_e k_f) e_f + \|e_f\| \delta_{robust4} - k'_e e_f \Omega_{robust4} \quad (50)$$

Substituting (47) into (50) gives.

$$\dot{V} \leq -e_f (k_d + k_e k_f) e_f \leq 0 \quad (51)$$

which is similar to the result in (45). Similarly, the convergence of the force error to zero can be further proven by the application of Barbalat's lemma [23]. The chattering effect can be reduced by replacing the discontinuous function, $\text{sgn}(e_f)$ in (47) with the continuous function, $\Omega_{robust4} = \frac{\delta_{robust4}}{k'_e} \left(\frac{e_f}{\delta_{ef} + |e_f|} \right)$, where δ_{ef} is a small constant value chosen between 0 to 0.1 [23].

2.6. Consideration of the Approximation Error with Unknown Upper Bound for Unknown Time-Varying Environment Location and Stiffness

Insufficient number of basis functions will lead to the approximation error in the FAT representation to be significant. If the upper bound of the approximation error is unknown, the error of the system can be proven to be uniformly ultimately bounded by the same target impedance in (34) and incorporating σ -modification terms. Using this method, it can be proven that the errors are uniformly ultimately bounded [23].

3. Impedance Controller

The control input force, F_{in} in (1) is necessary to bring the robotic system to reach the target impedance and finally achieve zero force and position tracking errors. Using the target impedance in (2), (7) and (33), this can be done by defining the augmented impedance error [20]-[23], Z as.

$$Z = \begin{cases} Z_f & \text{for free space in the force and position controllable directions} \\ Z_c & \text{for contact space in the force controllable direction with} \\ & \text{unknown constant stiffness and time-varying environment location} \\ Z_{cv} & \text{for contact space in the force controllable direction with} \\ & \text{unknown time-varying environment stiffness and location} \end{cases} \quad (52)$$

Under the contact space, for the force controllable direction and under unknown constant environment stiffness and time-varying environment location, the augmented impedance error, Z_c can be determined by rearranging (7) and multiplying the equation with matrix B_d^{-1} , yielding.

$$Z_c = B_d^{-1}(\theta_3 + \theta_4 + \theta_5 + \theta_6 + K_f E_f) + B_d^{-1}(K_d E' + \theta_1 + \theta_2) + \dot{E}', \quad (53)$$

where $E' = X - X_e'$ and $\dot{E}' \in \mathfrak{R}^{n \times 1}$ is its time derivative [20]-[23]. Similarly, the augmented impedance error, Z_{cv} to overcome both uncertain time-varying environment location and stiffness can be obtained by multiplying (33) with B_d^{-1} and rearranging the equation, [20]-[23].

$$Z_{cv} = B_d^{-1}(\theta_3 + \theta_4 + \theta_5 + \theta_{6v} + \theta_{7v} + K_f E_f) + B_d^{-1}(K_d E' + \theta_1 + \theta_2) + \dot{E}'. \quad (54)$$

Under the free space, Z_f in the position and force controllable directions this phase can be obtained from (2) by defining [53].

$$Z_f = \alpha E + \dot{E} + E_{fl} \quad (55)$$

where $M_d \dot{E}_{fl} + \eta M_d E_{fl} = E_f$. α and η are positive definite matrices [20]-[23], [53] chosen such that.

$$B_d - M_d \eta - M_d \alpha = 0, \quad K_d - M_d \alpha \eta - M_d \dot{\alpha} = 0 \quad (56)$$

The control input as in as in [53] is employed using the defined Z in (52), where.

$$F_{in} = F_e - KZ - (K_1 \|\ddot{X}_r\| + K_2 \|\dot{X}\| \|\dot{X}_r\| + K_3) \left(\frac{Z}{Z + \delta_z} \right) \quad (57)$$

And

$$Z = -\dot{X}_r + \dot{X} \quad (58)$$

The control parameters $K \in \mathfrak{R}^{n \times n}$, $K_1 \in \mathfrak{R}^{n \times n}$, $K_2 \in \mathfrak{R}^{n \times n}$, and $K_3 \in \mathfrak{R}^{n \times n}$ are definite positive diagonal matrices, in which their elements are chosen large enough such that $kM \geq \|M(X)\|$, $kC \|\dot{X}\| \geq \|C(X, \dot{X})\|$, $kG \geq \|G(X)\|$, $k_{1,i} \geq kM$, $k_{2,i} \geq kC$, $k_{3,i} \geq kG$, for $i = 1, 2, \dots, n$, [53]. $\dot{X}_r \in \mathfrak{R}^{n \times 1}$ is the reference velocity vector and $\delta_z \in \mathfrak{R}^{n \times 1}$ is the vector of positive constants incorporated to avoid input chattering problem. The detailed stability analysis for the augmented impedance error and control law (55)-(58) can be found in [53]. Fig. 1 shows the block diagram of the proposed Function Approximation Technique-based adaptive force-tracking impedance control for unknown time-varying environment.

4. Simulation Results and Discussions

A simulation study has been conducted to evaluate the effectiveness of the proposed controller in MATLAB environment. A 2 DOF robotic finger as in [20]-[23] is used in the simulation and the sampling time has been chosen as 0.001 s. The complete dynamic modelling of the robotic finger can be found in [23]. In this simulation, it is assumed that all the robotic finger parameters are known and available. During the free phase, $f_d = 0$ since the robotic finger has no contact with the environment. The robot is required to exert the desired force, f_d in x -direction on the environment's surface, while tracking a desired trajectory, y_d along y -axis in the contact space. The first 11 terms ($\beta_{(c)} = 11$) of Fourier Series have been selected to represent the estimation of the uncertainties, $\widehat{W}_{(c)} Z_{(c)}$. The period of the Fourier Series is set to be larger than the simulation time to ensure a valid range of time for the function to be orthonormal [20]-[23], [39]. The controller parameters have been tuned as.

$$K = \text{diag}[4200, 500], \quad K_1 = \text{diag}[10, 30], \quad K_2 = \text{diag}[20, 10], \quad K_3 = \text{diag}[7000, 3000], \quad (59)$$

$$B_d = \text{diag}[1270, 110], \quad K_d = \text{diag}[3000, 3000], \quad K_f = \text{diag}[10, 0], \quad \delta_z = [1, 1]^T,$$

$$M_d = \begin{cases} \text{diag}[1,1] & \text{(free space)} \\ \text{diag}[0,1] & \text{(contact space)} \end{cases}$$

And the values of α and η are directly calculated from (56) using the values of M_d, B_d and K_d in (56). The controller gains have been tuned manually. In the tuning process, these gains are adjusted first so that the shape of the actual force is as close as possible to the desired force. Then, the adaptation gains, $Q_{(\cdot)}$ are fine-tuned with the initial guess of identity matrices until the steady state error becomes zero. Increasing the value of each of the gains little by little will cause the actual result to be closer to the desired output. However, if the value is too high, it will cause the resulting force to vibrate. When this occur, the value of the gain needs to be reduced to the value that gives the closest output to the desired force and then, the gain needs to be fine-tuned. This tuning process is repeated for the rest of the gains until the best result is achieved. No optimization algorithm has been employed to automate the tuning process in this work.

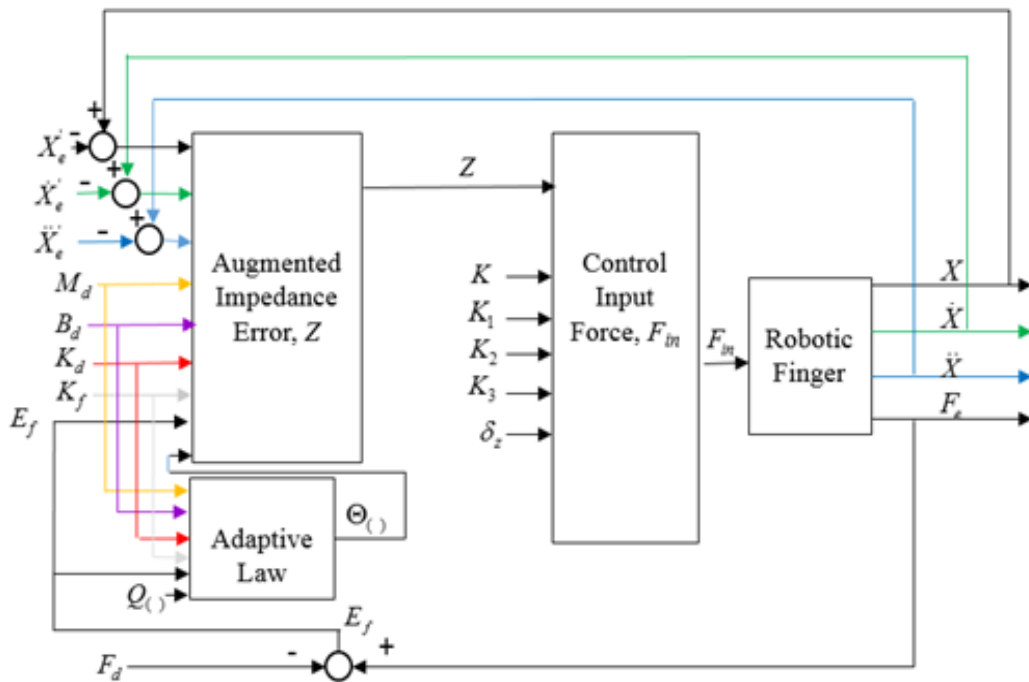


Fig. 1. Block diagram of the proposed controller

4.1. Unknown Constant Environment Stiffness and Time-Varying Environment Location

In this simulation, the proposed target impedance (8) and update laws (10) are tested to overcome the uncertain constant environment stiffness and time-varying location. The real environment location, x_e can be expressed as.

$$x_e = 0.004 \sin \frac{2\pi(t-0.0833)}{2/3} + 0.0375 \text{ m} \quad (60)$$

x_e is initially estimated as a flat environment where, $x_e' = 0.042$ m because it is assumed that precise information of this quantity to be unavailable priori. Two values of true environment stiffness are tested, which are $k_e = 40000\text{N/m}$ and $k_e = 10000\text{N/m}$, and these values are initially estimated as $k_e' = 50000\text{N/m}$ and $k_e' = 20000\text{N/m}$ respectively. The adaptation gain for $k_e = 40000\text{N/m}$ have been tuned as $Q_1^{-1} = 10^2 I_{11}$, $Q_2^{-1} = I_{11}$, $Q_3^{-1} = 10 I_{11}$, $Q_4^{-1} = I_{11}$, $Q_6^{-1} = 1$ and for $k_e = 10000\text{N/m}$, $Q_1^{-1} = 10 I_{11}$, $Q_2^{-1} = I_{11}$, $Q_3^{-1} = I_{11}$, $Q_4^{-1} = 10^{-1} I_{11}$, $Q_6^{-1} = 1$. The force and position tracking response are shown in Fig. 2 and Fig. 3 respectively. From the results, it can be seen the robot has successfully tracked the desired force and position under the proposed strategy. It has applied the required amount of force on the environment while precisely follows the required path along y -direction, despite the time-varying uncertainties in the environment stiffness and location.

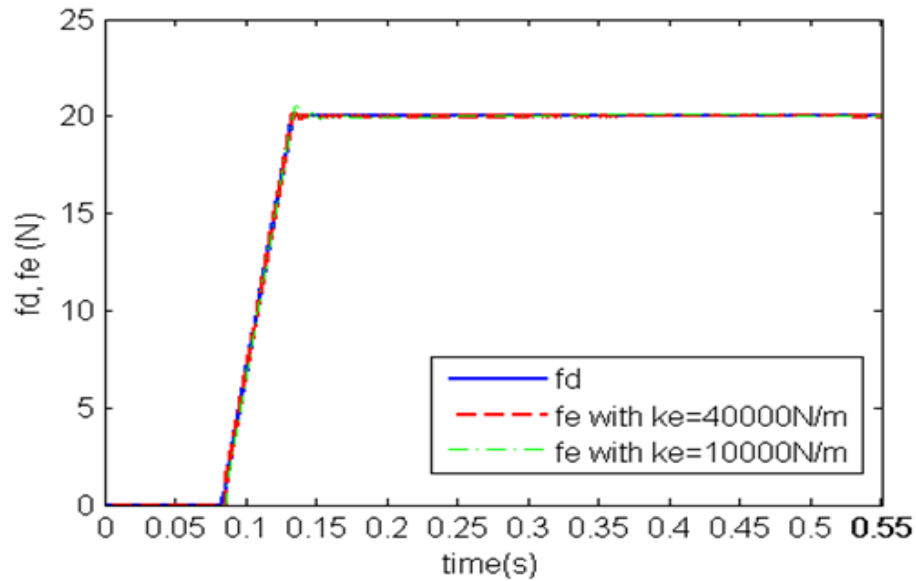


Fig. 2. Force-tracking response in x -direction for $k_e=40000$ N/m and $k_e=10000$ N/m

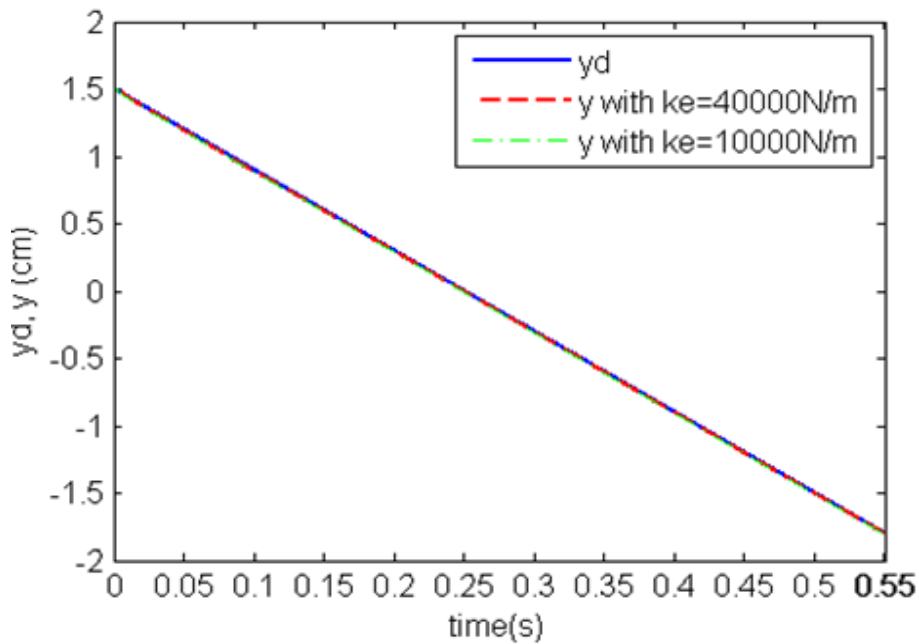


Fig. 3. Position tracking response in y -direction for $k_e=40000$ N/m and $k_e=10000$ N/m

4.1.1. Effect of the Initial Environment Stiffness Estimate, k'_e

In the proposed approach, the designer has to select the value of the initial environment stiffness estimation, k'_e before the control algorithm can be implemented. In this section, the effect of k'_e selection on the overall performance of the control strategy is investigated. The real value of k_e is set as 40000 N/m. The proposed algorithm (8) and (10) are tested under different values of k'_e , where $k'_e = 20000$ N/m, 50000 N/m, 60000 N/m, 80000 N/m, 100000 N/m and 120000 N/m.

Fig. 4 illustrates the force response under different values of k'_e . The result demonstrates that good force-tracking performances can be achieved with a high variation in k'_e . The robotic finger has successfully applied the required force with less than 0.5 N error even if k'_e is selected lower than or twice higher than k_e . Therefore, it can be concluded that a wide range of k'_e can be chosen to attain an excellent force-tracking result. This may be attributed to the effectiveness of the developed control

law that can adapt to the uncertainties in the environmental stiffness whilst ensuring the stability of the system by Lyapunov theory. However, the root mean square error (RMSE) of the force increases when the initial guess is farther from the actual value. Nevertheless, this value is still very low as can be seen in Fig. 4. The effect of the selection of x'_e and adaptation gain, Q_C^{-1} on the system performance can be found in [23].

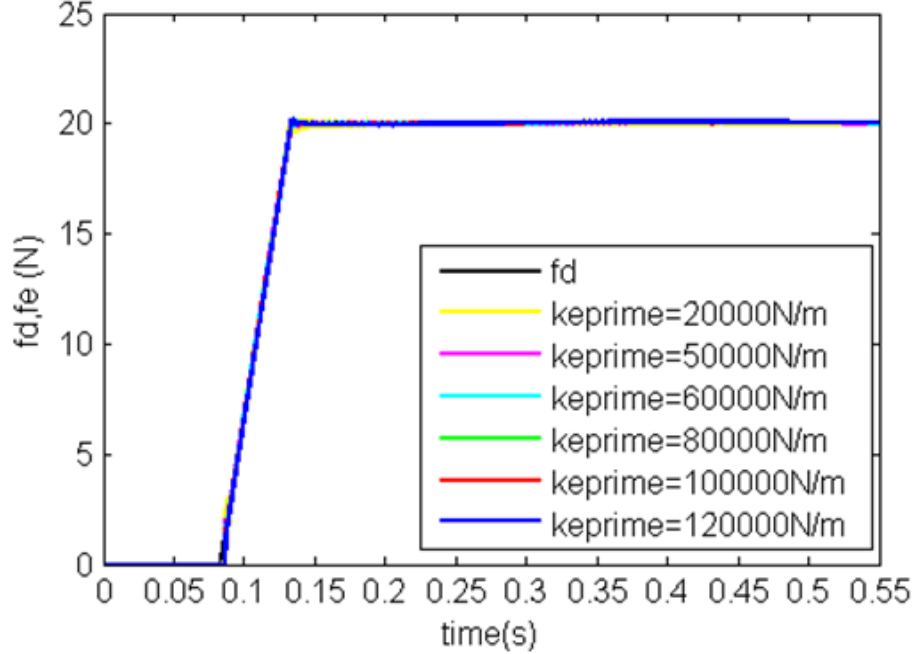


Fig. 4. Force-tracking response in x -direction for different values of k'_e

4.2. Unknown Time-Varying Environment Location and Stiffness

4.2.1. Case 1: Sinusoidally Time Varying Unknown Location and Stiffness

In this simulation test, the effectiveness of the proposed target impedance (34) in compensating unknown time-varying environment parameters is verified. The real but unknown values of k_e and x_e have been set to be varying sinusoidally with time as the robot moves along the y -axis, where.

$$k_e = 25000 + 10000 \sin \frac{2\pi(t-0.0833)}{0.5} \text{ N/m}, \quad (61)$$

$$x_e = 0.004 \sin \frac{2\pi(t-0.0833)}{2/3} + 0.0375 \text{ m}. \quad (62)$$

Similarly, k_e and x_e are assumed to be unknown precisely in advance. For simplicity, their initial values are estimated roughly as a constant, where $k'_e = 50000 \text{ N/m}$ and $x'_e = 0.042 \text{ m}$. The robot is set to apply a sinusoidally varying reference force, f_d on the environment surface, where.

$$f_d = \begin{cases} 0 \text{ N} & 0 \text{ s} \leq t \leq 0.08 \text{ s} \\ 400(t - 0.08) \text{ N} & 0.08 \text{ s} \leq t \leq 0.13 \text{ s} \\ 25 + 6 \sin((2\pi t - 0.08)/0.25) \text{ N} & t > 0.13 \text{ s} \end{cases} \quad (63)$$

while tracking the desired trajectory, y_d . The same control parameters as in (59) have been employed and Q_C^{-1} have been chosen as $Q_1^{-1} = 10I_{11}$, $Q_2^{-1} = I_{11}$, $Q_3^{-1} = 10I_{11}$, $Q_4^{-1} = 10^{-1}I_{11}$, $Q_{6v}^{-1} = 10^{-1}I_{11}$, $Q_{7v}^{-1} = I_{11}$.

The force and position responses in Fig. 5 and Fig. 6 respectively demonstrate that high force-tracking accuracy and excellent position following result can be achieved under the proposed target impedance even though the accurate environment parameters are unknown. The result also shows that

the proposed technique is also capable of tracking not only constants but also time-varying desired force. In Fig. 6, the true environment location is represented by the blue line and it is assumed to be unknown precisely beforehand. Therefore, it is initially estimated as a constant, x_e' , which is indicated by the straight green line. The black line represents the reference trajectory, x_d . In the free space, x_d can be specified without considering the environment parameters. After the robot has become in contact with the environment, x_d can be calculated using (5) and the exact value of k_e and x_e to produce the accurate f_d . From Fig. 6, it can be seen that, in the constraint-motion phase, the robot produces the same actual trajectory, x_e as the calculated trajectory, x_d in (5), which agrees with the force response in Fig. 5. The system is able to exert the desired amount of force while tracking the position precisely regardless of the environmental shape (location) and stiffness.

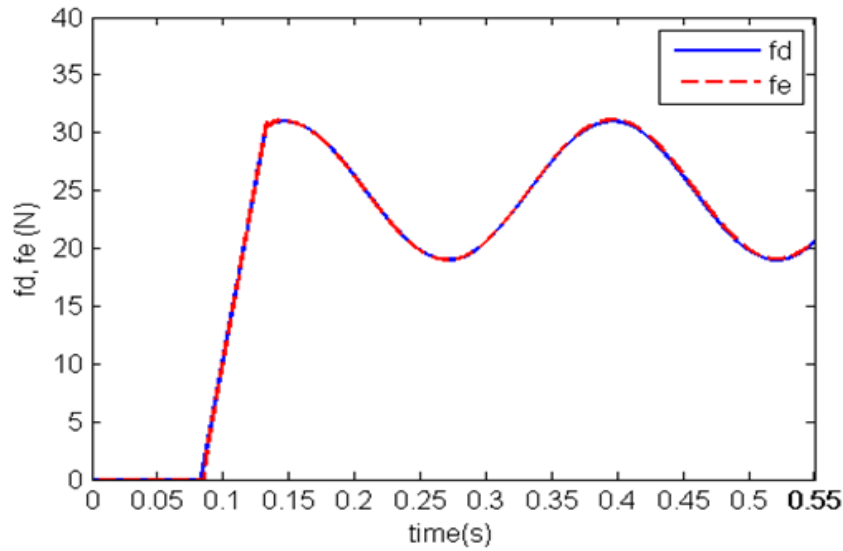


Fig. 5. Force-tracking response in x -direction for f_d in (63)

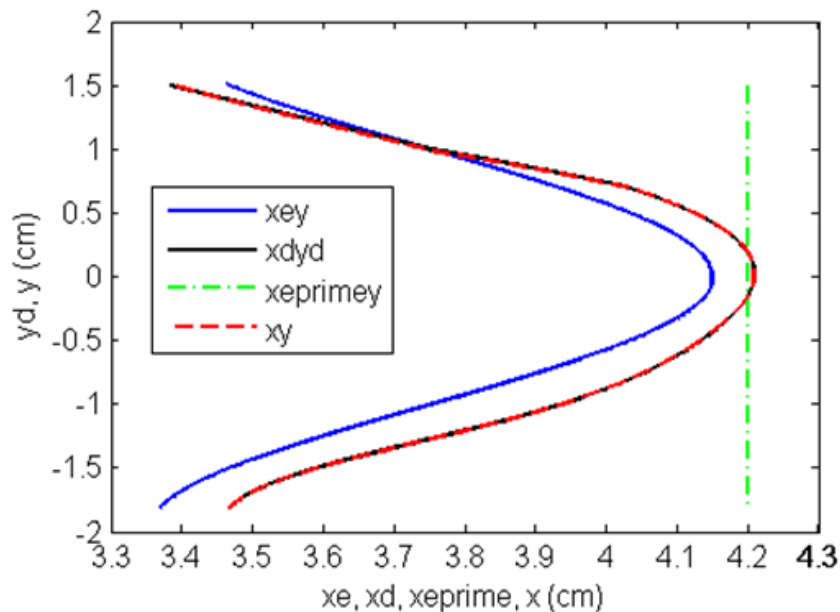


Fig. 6. Position response in Cartesian space for f_d in (63)

4.2.2. Case 2: Time Varying Desired Force

The simulation has been repeated with the same unknown k_e , x_e and control parameters, but with different f_d to check the performance of the formulated controller under various time varying forces. The desired force has been set as.

$$f_d = 25 + 12 \sin((2\pi t - 0.08)/0.5) \text{ N} \quad t > 0.13 \text{ s} \quad (64)$$

And

$$f_d = \begin{cases} 0 \text{ N} & 0 \text{ s} \leq t \leq 0.08 \text{ s} \\ 400(t - 0.08) \text{ N} & 0.08 \text{ s} \leq t \leq 0.1 \text{ s} \\ 10 \text{ N} & 0.1 \text{ s} \leq t \leq 0.2 \text{ s} \\ 400(t - 0.22) \text{ N} & 0.2 \text{ s} \leq t \leq 0.22 \text{ s} \\ 22.3 \text{ N} & 0.22 \text{ s} \leq t \leq 0.4 \text{ s} \\ -200(t - 0.4) + 22.3 \text{ N} & 0.4 \text{ s} \leq t \leq 0.42 \text{ s} \\ 16.5 \text{ N} & t > 0.42 \text{ s} \end{cases} \quad (65)$$

Fig. 7 shows the force error, e_f for the time-varying desired force in (64) and (65). The results exhibit that the error is almost zero for both cases. Therefore, the control law is effective in driving the system to achieve the required force although it is not constant and varies with respect to time.

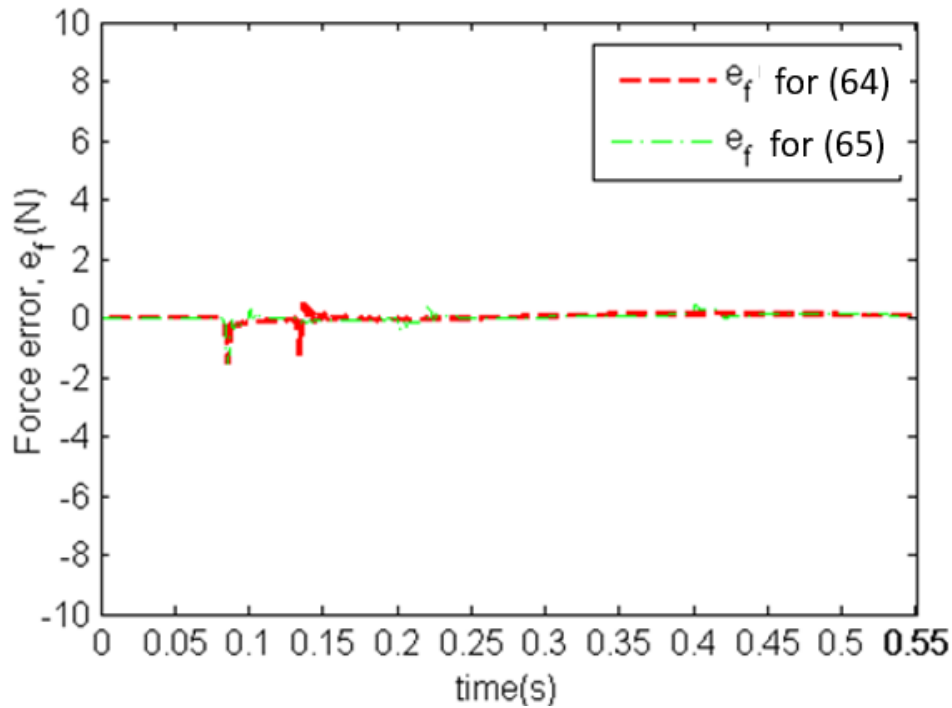


Fig. 7. Force error for the desired f_d in (64) and (65)

4.2.3. Case 3: Non-continuous Time Varying Unknown Environment Location and Stiffness

In this case, the performance of the proposed control technique (34) is tested on a non-continuous k_e and x_e variation, where.

$$k_e = \begin{cases} 40000 \text{ N/m} & 0 \text{ s} \leq t \leq 0.15 \text{ s} \\ -30000t + 8500 \text{ N/m} & 0.15 \text{ s} \leq t \leq 0.25 \text{ s} \\ 10000 \text{ N/m} & 0.25 \text{ s} \leq t \leq 0.35 \text{ s} \\ 50000t - 16500 \text{ N/m} & 0.35 \text{ s} \leq t \leq 0.45 \text{ s} \\ 60000 \text{ N/m} & t \geq 0.45 \text{ s} \end{cases} \quad (66)$$

$$x_e = \begin{cases} 0.0375 \text{ m} & 0 \text{ s} \leq t \leq 0.25 \text{ s} \\ -5 \times 10^{-4}t + 5 \times 10^{-4} \text{ m} & 0.25 \text{ s} \leq t \leq 0.30 \text{ s} \\ 0.0350 \text{ m} & 0.30 \text{ s} \leq t \leq 0.35 \text{ s} \\ 2 \times 10^{-4}t + 2.8 \times 10^{-4} \text{ m} & 0.35 \text{ s} \leq t \leq 0.40 \text{ s} \\ 0.0360 \text{ m} & t \geq 0.40 \text{ s} \end{cases} \quad (67)$$

And their initial guess are set as $k'_e = 50000\text{N/m}$, $x'_e = 0.042\text{ m}$. The value of K has been modified to $K = \text{diag}[8000,500]$ and the rest of the controller parameters are similar as (59). The adaptation gains have been selected as $Q_1^{-1} = 10^3 I_{11}$, $Q_2^{-1} = 10 I_{11}$, $Q_3^{-1} = 10 I_{11}$, $Q_4^{-1} = 10^2 I_{11}$, $Q_{6v}^{-1} = 10^2 I_{11}$, $Q_{7v}^{-1} = 10^2 I_{11}$.

From Fig. 8 and Fig. 9, it can be observed that the actual force exerted on the environment, f_e has followed the commanded force, f_d accurately. The robot has tracked the desired position precisely and has successfully accomplished the required task. In the contact space, it has produced the same trajectory as the calculated x_d , which is determined based on the actual environment position and stiffness information. Therefore, it can be deduced that the developed control law is effective in compensating for the unknown time-varying environment stiffness and location. Fig. 9 also shows that the resulted x_d in the contact space is more complicated than Case 1 due to the real shape of the environment in (67) and the variation in the environment stiffness in (66).

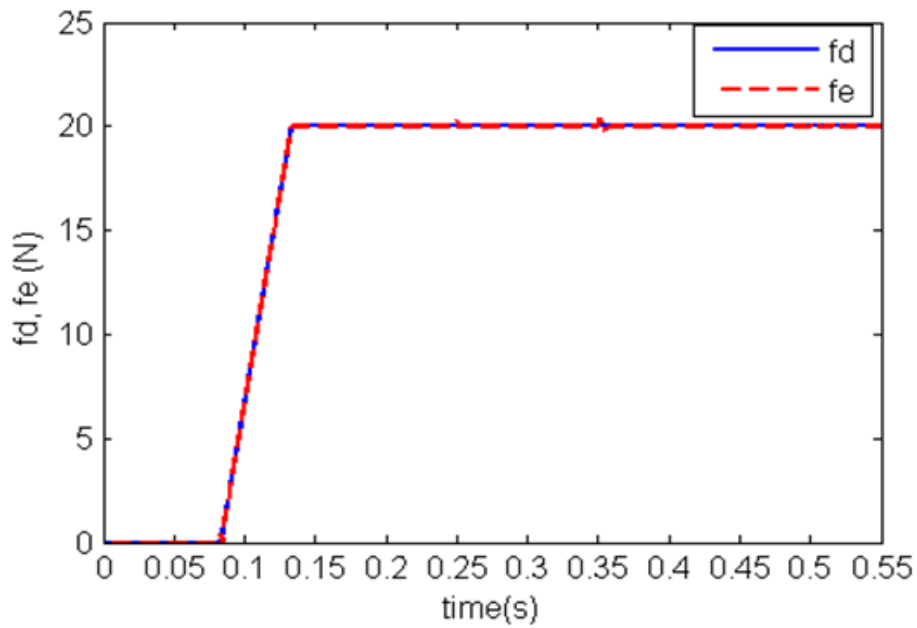


Fig. 8. Force-tracking response in x-direction for Case 3

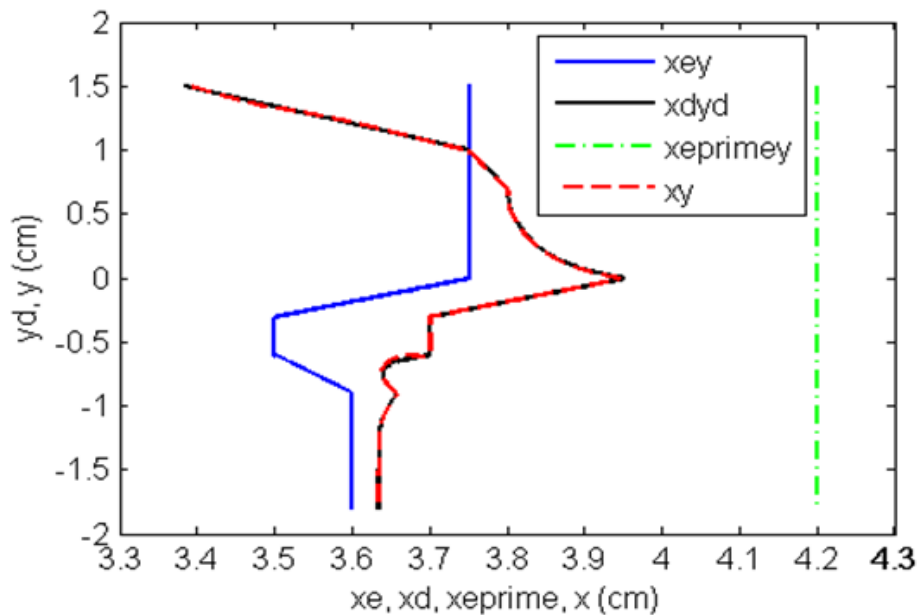


Fig. 9. Position response in Cartesian Space for Case 3

4.2.4. Case 4: Constant Unknown Environment Location and Stiffness

In this case, the simulation has been carried out to investigate whether the proposed controller (27) can provide a similar excellent performance if the robot is working under uncertain constant environment location and stiffness, even though the strategy is designed for uncertain time-varying environment parameters. The true values of k_e and x_e are set as constants where $k_e = 40000$ N/m and $x_e = 0.0375$ m. Since this information is assumed to be unavailable a priori, they are initially estimated as $k'_e = 50000$ N/m and $x'_e = 0.042$ m. The same control parameters as in (59) have been applied and $Q_{(.)}$ have been adjusted to $Q_1^{-1} = 10^{-1}I_{11}$, $Q_2^{-1} = 10^{-1}I_{11}$, $Q_3^{-1} = 10^{-1}I_{11}$, $Q_4^{-1} = 10^{-1}I_{11}$, $Q_{6v}^{-1} = I_{11}$, $Q_{7v}^{-1} = I_{11}$.

From the results illustrated in Fig. 10 and Fig. 11, it can be observed that the formulated approach has successfully overcome the unknown constant environment stiffness and shape problem, although it is originally derived for uncertain time-varying environment parameters. An excellent force-tracking performance can be achieved in this case since the Fourier Series that is utilized as the FAT expression can also represent constant functions.

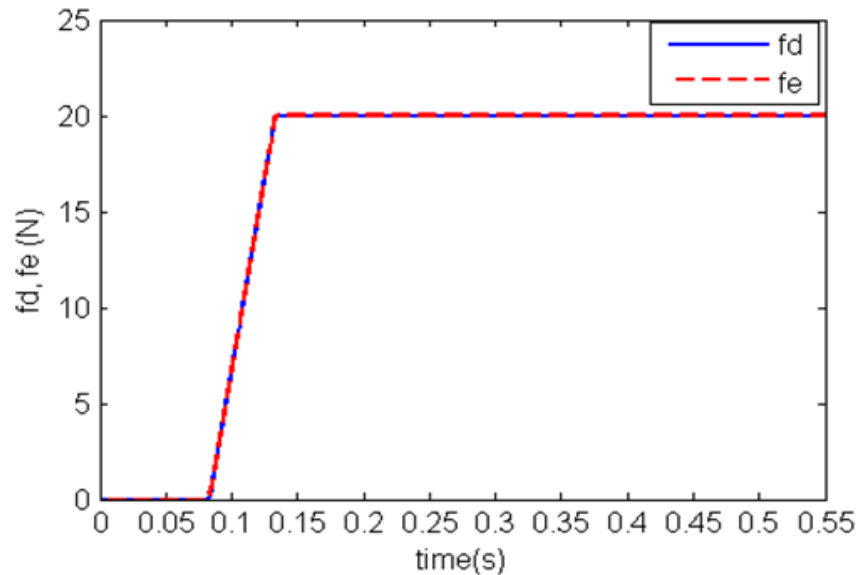


Fig. 10. Force-tracking response in x -direction for Case 4

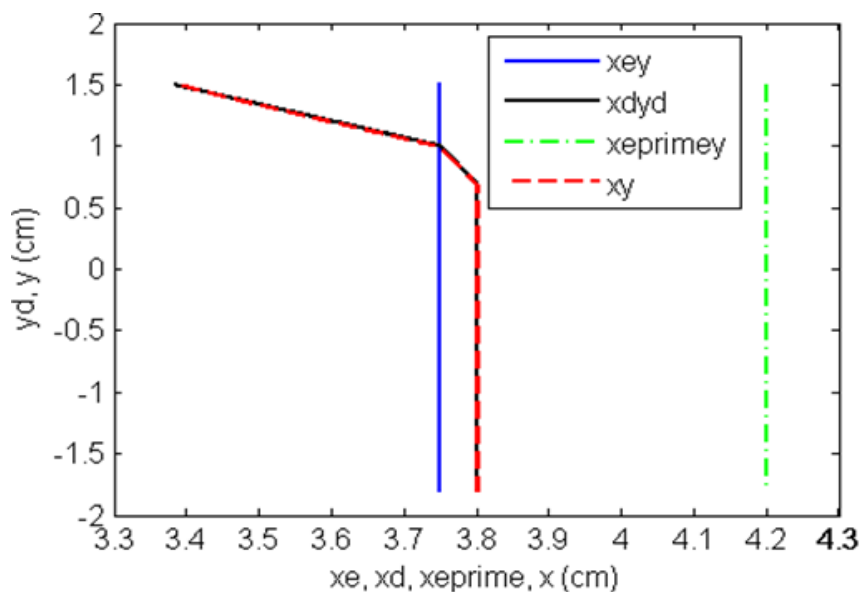


Fig. 11. Position response in Cartesian space for Case 4

4.3. Consideration on the Approximation Error with Known Upper Bound for Unknown Time-Varying Environment Location and Constant Environment Stiffness

From Fig. 12, it can be seen that the force error which is due to the approximation error in the Fourier Series can be decreased by employing the modified target impedance (26), where $\delta_{robust3} = 50$. The chattering effect in the $sgn(e_f)$ function in (27) has been reduced by replacing it with the well-known continuous function, $\frac{e_f}{\delta_{ef} + |e_f|}$, where δ_{ef} has been set as 0.04.

4.4. Consideration on the Approximation Error with Known Upper Bound for Unknown Time-Varying Environment Location and Stiffness

Fig. 13 shows the force response in x -direction under the modified target impedance (46), with an insufficient numbers of basis functions. The value of $\delta_{robust4}$ is set to be 3×10^7 and the value of δ_{ef} is tuned to be 0.01. The figure demonstrates an accurate result can still be obtained by implementing the modified target impedance in (46) even though the number of basis function is low.

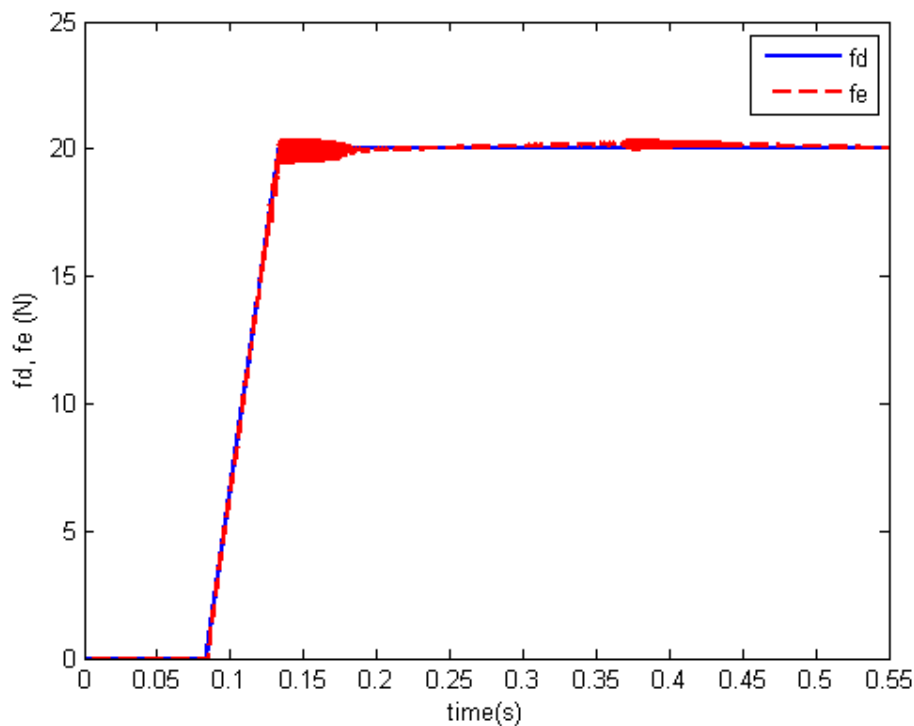


Fig. 12. Force response in x -direction using target impedance (26) and continuous function $\frac{e_f}{\delta_{ef} + |e_f|}$

4.5. Discussion

The simulation results show that the controller is effective in providing an accurate force tracking in the event of uncertain time-varying environment stiffness and location (geometrical shape). The simulations tests have been conducted on various environment surfaces and stiffness, for achieving constant and time-varying reference forces. The effect of the initial environment stiffness estimate, k_e' has also been studied where a high variation in k_e' can be used as the initial guess without compromising the output performance. The results also illustrate that a precise tracking outcome can still be attained by implementing the modified target impedances (26) and (46) even though the number of basis function is low, and the approximation error cannot be neglected. In the proposed control law, the derivative of the force feedback signal that is usually noisy is not required and the switching of the stiffness gain in the target impedance that may lead to instability is unnecessary. However, this study is limited to simulation tests only. The practicality and reliability of the system under real world need to verified though hardware experimental tests to ensure the efficacy of the

proposed approach in comparison to existing methods. The proposed control algorithm also may involve a high computational time that may compromise its performance in the real time application since its implementation involves a lot of mathematical calculations. The alternatives to reduce its computational time and effort such as the utilization of a more efficient basis function in the FAT expression may be explored. In this study, it is also assumed that the dynamic model and parameters of the robotic finger are known. Even though there are many existing studies on overcoming the uncertain robot dynamics and external disturbances using FAT, it would be valuable to study the effectiveness of the proposed controller in compensating the combination of time-dependent unknowns in the plant dynamics, external disturbances and noise, environment stiffness and environment location.

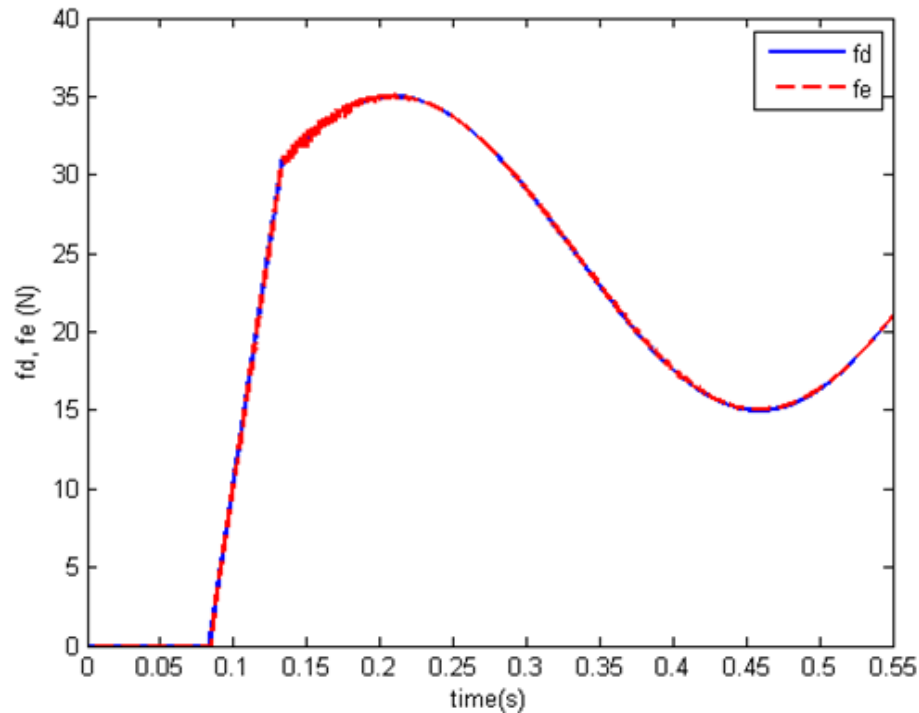


Fig. 13. Force response in x -direction using target impedance (46) with the consideration on the approximation error, ε_c under known upper bound

5. Conclusion

A FAT-based adaptive impedance control strategy has been developed for uncertain non-constant environment parameters and applied on a robotic finger. The formulation of the controller with the consideration on the approximation error with known upper bound has also been presented in this paper. The simulation results under various environment stiffness and locations have validated the effectiveness of the proposed controller in driving the robot to achieve excellent force and position tracking performances under limited information of the environment parameters. The stability of the controller has been guaranteed by Lyapunov stability theory. The control law does not require the derivative of the measured force feedback signal and the switching of the stiffness gain in as the finger travels from noncontact to contact spaces. These features contribute to the practicality and robustness of the proposed control law since it avoids the use of the force signal's derivative that contains high noise and avoids instability that may result from the switching of the stiffness gain. The proposed controller also enables the system to track time-varying desired forces precisely instead of limiting the force tracking capability to constant forces only. This capability can enhance the robot's adaptability and versatility in dynamic environments. Future works involve investigating the performance, practicality and reliability of the proposed controller in the real world implementation by conducting the hardware experimental tests. The alternatives to reduce its computational time and effort, such as

the application of a simpler basis function to reduce its computational effort in ensuring its performance in the real-time operation need to be further studied. The utilization of the proposed controller in compensating the combination of time-dependent unknowns in the plant dynamics, external disturbances, environment stiffness and environment location simultaneously may also be explored in the future work. Further research on the adoption or combination of the proposed control law with other robust control techniques in other scenarios or robotic systems also may also be conducted to solve for different types of uncertainties or variations in the system.

Author Contribution: Norsinnira Zainul Azlan contributed in formulating the control law, conducting the simulation tests and writing the paper. Hiroshi Yamaura provided some input on the control law formulation and simulation studies. Iswanto Suwarno contributed in the article writing. All authors read and approved the final paper.

Funding: The authors would like to thank International Islamic University Malaysia for supporting this research under the grant number: P-RIGS18-019-0019.

Conflicts of Interest: The authors declare no conflict of interest.

References

- [1] N. Hogan, "Impedance control: An approach to manipulation parts I, II and III.," *Journal of Dynamic Systems, Measurements and Control*, vol. 107, no. 1, pp. 17-24, 1985, <https://doi.org/10.1115/1.3140701>.
- [2] M. H. Raibert and J. J. Craig, "Hybrid position/ force control of manipulators," *Journal of Dynamic Systems, Measurements and Control*, vol. 103, no. 2, pp. 126-133, 1981, <https://doi.org/10.1115/1.3139652>.
- [3] H. Li, L. Cheng, N. Sun and R. Cao, "Design and Control of an Underactuated Finger Exoskeleton for Assisting Activities of Daily Living," *IEEE/ASME Transactions on Mechatronics*, vol. 27, no. 5, pp. 2699-2709, 2022, <https://doi.org/10.1109/TMECH.2021.3120030>.
- [4] Z. Xu, S. Li, X. Zhou, S. Zhou, T. Cheng and Y. Guan, "Dynamic Neural Networks for Motion-Force Control of Redundant Manipulators: An Optimization Perspective," *IEEE Transactions on Industrial Electronics*, vol. 68, no. 2, pp. 1525-1536, 2021, <https://doi.org/10.1109/TIE.2020.2970635>.
- [5] C. Zeng, S. Li, Z. Chen, C. Yang, F. Sun and J. Zhang, "Multifingered Robot Hand Compliant Manipulation Based on Vision-Based Demonstration and Adaptive Force Control," *IEEE Transactions on Neural Networks and Learning Systems*, vol. 34, no. 9, pp. 5452-5463, 2023, <https://doi.org/10.1109/TNNLS.2022.3184258>.
- [6] H. Ochoa and R. Cortesão, "Impedance Control Architecture for Robotic-Assisted Mold Polishing Based on Human Demonstration," *IEEE Transactions on Industrial Electronics*, vol. 69, no. 4, pp. 3822-3830, 2022, <https://doi.org/10.1109/TIE.2021.3073310>.
- [7] G. Li, X. Chen, J. Yu and J. Liu, "Adaptive Neural Network-Based Finite-Time Impedance Control of Constrained Robotic Manipulators With Disturbance Observer," *IEEE Transactions on Circuits and Systems II: Express Briefs*, vol. 69, no. 3, pp. 1412-1416, 2022, <https://doi.org/10.1109/TCSII.2021.3109257>.
- [8] X. Zhao, S. Han, B. Tao, Z. Yin and H. Ding, "Model-Based Actor-Critic Learning of Robotic Impedance Control in Complex Interactive Environment," *IEEE Transactions on Industrial Electronics*, vol. 69, no. 12, pp. 13225-13235, 2022, <https://doi.org/10.1109/TIE.2021.3134082>.
- [9] X. Jin, "Formation-Based Decentralized Iterative Learning Cooperative Impedance Control for a Team of Robot Manipulators," *IEEE Transactions on Systems, Man, and Cybernetics: Systems*, vol. 53, no. 2, pp. 872-881, 2023, <https://doi.org/10.1109/TSMC.2022.3189661>.
- [10] Y. Huo, P. Li, D. Chen, Y. -H. Liu and X. Li, "Model-Free Adaptive Impedance Control for Autonomous Robotic Sanding," *IEEE Transactions on Automation Science and Engineering*, vol. 19, no. 4, pp. 3601-3611, 2022, <https://doi.org/10.1109/TASE.2021.3126743>.

-
- [11] T. Goyal, S. Hussain, E. Martinez-Marroquin, N. A. T. Brown and P. K. Jamwal, "Impedance Control of a Wrist Rehabilitation Robot Based on Autodidact Stiffness Learning," *IEEE Transactions on Medical Robotics and Bionics*, vol. 4, no. 3, pp. 796-806, 2022, <https://doi.org/10.1109/TMRB.2022.3194528>.
- [12] Y. Deng, G. Wang, X. Yue and K. Zhou, "A Review of Robot Grinding and Polishing Force Control Mode," *2022 IEEE International Conference on Mechatronics and Automation (ICMA)*, pp. 1413-1418, 2022, <https://doi.org/10.1109/ICMA54519.2022.9855998>.
- [13] C. Zhang, N. Sun, Y. Chen, Z. Qiu, W. Sang and Y. Fang, "Error Constrained Hybrid Force/Position Control of a Grinding Robot," *2021 IEEE International Conference on Real-time Computing and Robotics (RCAR)*, pp. 101-106, 2021, <https://doi.org/10.1109/RCAR52367.2021.9517684>.
- [14] M. Adinehvand, C. Y. Lai and R. Hoseinnezhad, "Barrier-Lyapunov -Function-Based Backstepping Adaptive Hybrid Force/Position Control for Manipulator with Force and Position Constraints," *2021 American Control Conference (ACC)*, pp. 2266-2271, 2021, <https://doi.org/10.23919/ACC50511.2021.9483300>.
- [15] O. K. Adak, B. Bahceci and K. Erbatur, "Hybrid Force-Motion Control for One-Legged Robot in Operational Space," *2021 IEEE/ASME International Conference on Advanced Intelligent Mechatronics (AIM)*, pp. 905-910, 2021, <https://doi.org/10.1109/AIM46487.2021.9517455>.
- [16] H. C. Schubert, "Impedance Control of Flexible Macro/Mini Manipulators," *PhD Dissertation, Dept. Aeronautics & Astronautics, Stanford University*, 2000, <https://web.stanford.edu/group/arl/cgi-bin/drupal/sites/default/files/public/publications/Schubert%202000.pdf>.
- [17] H. Seraji and R. Colbaugh, "Force tracking in impedance control," *[1993] Proceedings IEEE International Conference on Robotics and Automation*, vol. 2, pp. 499-506, 1993, <https://doi.org/10.1109/ROBOT.1993.291908>.
- [18] S. Jung, T. C. Hsia and R. G. Bonitz, "Force tracking impedance control of robot manipulators under unknown environment," *IEEE Transactions on Control Systems Technology*, vol. 12, no. 3, pp. 474-483, 2004, <https://doi.org/10.1109/TCST.2004.824320>.
- [19] K. Lee and M. Buss, "Force-tracking impedance control with variable target stiffness," *Proceedings of the International Federation of Automatic Control*, vol. 41, no. 2, pp. 6751- 6756, 2008, <https://doi.org/10.3182/20080706-5-KR-1001.01144>.
- [20] N. Z. Azlan and H. Yamaura, "Function Approximation Technique based Adaptive Impedance Control for Uncertain Environment," *International Journal of Mechanical and Mechatronics Engineering*, vol. 6, no. 8, pp. 1538-1543, 2012, <http://irep.iium.edu.my/47726/>.
- [21] N. Z. Azlan and H. Yamaura, "Adaptive Impedance Control for Unknown Time-Varying Environment Position and Stiffness," *International Journal of Mechanical and Mechatronics Engineering*, vol. 7, no. 2, pp. 283-289, 2013, <http://irep.iium.edu.my/47712/>.
- [22] N. Z. Azlan and H. Yamaura, "Adaptive Impedance Control for Unknown Non-Flat Environment," *International Journal of Mechanical and Mechatronics Engineering*, vol. 7, no. 2, pp. 191-196, 2013, <https://irep.iium.edu.my/47730/>.
- [23] N. Z. Azlan, "Mechanical design and FAT-based adaptive impedance control of robotic finger," *Ph.D. dissertation, Department of Mechanical and Control Engineering, Tokyo Institute of Technology*, 2013, <https://ci.nii.ac.jp/naid/500002471272>.
- [24] O. S. Ajani and S. F. M. Assal, "Hybrid Force Tracking Impedance Control-Based Autonomous Robotic System for Tooth Brushing Assistance of Disabled People," *IEEE Transactions on Medical Robotics and Bionics*, vol. 2, no. 4, pp. 649-660, 2020, <https://doi.org/10.1109/TMRB.2020.3030317>.
- [25] H. Wang and Y. Xie, "Adaptive Jacobian force/position tracking control of robot manipulators in compliant contact with an uncertain surface," *Advanced Robotics*, vol. 23, no. 1-2, pp. 165-183, 2009, <https://doi.org/10.1163/156855308X392726>.
- [26] C. Yang, G. Peng, Y. Li, R. Cui, L. Cheng and Z. Li, "Neural Networks Enhanced Adaptive Admittance Control of Optimized Robot-Environment Interaction," *IEEE Transactions on Cybernetics*, vol. 49, no. 7, pp. 2568-2579, 2019, <https://doi.org/10.1109/TCYB.2018.2828654>.
-

-
- [27] X. Zhang and M. B. Khamesee, "Adaptive Force Tracking Control of a Magnetically Navigated Microrobot in Uncertain Environment," *IEEE/ASME Transactions on Mechatronics*, vol. 22, no. 4, pp. 1644-1651, 2017, <https://doi.org/10.1109/TMECH.2017.2705523>.
- [28] H. Liu, B. Zhou, Y. Gan and X. Ma, "Compliant control based on impedance principle under unknown environmental stiffness," *WRC Symposium on Advanced Robotics and Automation (WRC SARA)*, pp. 341-346, 2019, <https://doi.org/10.1109/WRC-SARA.2019.8931951>.
- [29] H. Cao, X. Chen, Y. He and X. Zhao, "Dynamic Adaptive Hybrid Impedance Control for Dynamic Contact Force Tracking in Uncertain Environments," *IEEE Access*, vol. 7, pp. 83162-83174, 2019, <https://doi.org/10.1109/ACCESS.2019.2924696>.
- [30] H. Wakamatsu, M. Yamanoi and K. Tatsuno, "Adaptive force control of robot arm with estimation of environmental stiffness," *2010 International Symposium on Micro-NanoMechatronics and Human Science*, pp. 226-231, 2010, <https://doi.org/10.1109/MHS.2010.5669556>.
- [31] L. J. Love and W. J. Book, "Environment estimation for enhanced impedance control," *Proceedings of 1995 IEEE International Conference on Robotics and Automation*, vol. 2, pp. 1854-1859, 1995, <https://doi.org/10.1109/ROBOT.1995.525537>.
- [32] Y. Li, S. S. Ge and K. P. Tee, "Adaptive impedance control for natural human-robot collaboration," *Proceedings of the Workshop at SIGGRAPH Asia*, pp. 91-96, 2012, <https://doi.org/10.1145/2425296.2425313>.
- [33] S. Kim, J. -P. Kim and J. Ryu, "Adaptive Energy-Bounding Approach for Robustly Stable Interaction Control of Impedance-Controlled Industrial Robot With Uncertain Environments," *IEEE/ASME Transactions on Mechatronics*, vol. 19, no. 4, pp. 1195-1205, 2014, <https://doi.org/10.1109/TMECH.2013.2276935>.
- [34] S. S. Ge, Y. Li and C. Wang, "Impedance adaptation for optimal robot-environment interaction," *International Journal of Control*, vol. 87, no. 2, pp. 249-263, 2014, <https://doi.org/10.1080/00207179.2013.827799>.
- [35] B. Komati, C. Cleve and P. Lutz, "Force tracking impedance control with unknown environment at the microscale," *IEEE International Conference on Robotics and Automation (ICRA)*, pp. 5203-5208, 2014, <https://doi.org/10.1109/ICRA.2014.6907623>.
- [36] Y. Xie, D. Sun, C. Liu and S. H. Cheng, "An adaptive impedance force control approach for robotic cell microinjection," *IEEE/RSJ International Conference on Intelligent Robots and Systems*, pp. 907-912, 2008, <https://doi.org/10.1109/IROS.2008.4650824>.
- [37] Y. Li, C. Yang and S. S. Ge, "Learning compliance control of robot manipulators in contact with the unknown environment," *2010 IEEE International Conference on Automation Science and Engineering*, pp. 644-649, 2010, <https://doi.org/10.1109/COASE.2010.5584228>.
- [38] C. S. Tzafestas, N. K. M'sirdi and N. Manamani, "Adaptive impedance control applied to a pneumatic legged robot," *Journal of Intelligent and Robotic Systems*, vol. 20, pp. 105-129, 1997, <https://doi.org/10.1023/A:1007987608963>.
- [39] A. C. Huang and M. C. Chien, "Adaptive Control of Robot Manipulators: A Unified Regressor-Free Approach," *Singapore: World Scientific Publishing*, p. 276, 2010, <https://doi.org/10.1142/7760>.
- [40] Y. Bai, M. Svinin, Y. Wang and E. Magid, "Function Approximation Technique Based Control for a Class of Nonholonomic Systems," *2020 IEEE/SICE International Symposium on System Integration (SII)*, pp. 283-288, 2020, <https://doi.org/10.1109/SII46433.2020.9026292>.
- [41] Y. Bai, Y. Wang, M. Svinin, E. Magid and R. Sun, "Function Approximation Technique Based Immersion and Invariance Control for Unknown Nonlinear Systems," *IEEE Control Systems Letters*, vol. 4, no. 4, pp. 934-939, 2020, <https://doi.org/10.1109/LCSYS.2020.2997600>.
- [42] Y. Bai, Y. Wang, M. Svinin, E. Magid and R. Sun, "Adaptive Multi-Agent Coverage Control With Obstacle Avoidance," *IEEE Control Systems Letters*, vol. 6, pp. 944-949, 2022, <https://doi.org/10.1109/LCSYS.2021.3087609>.
-

- [43] D. Ebeigbe, T. Nguyen, H. Richter and D. Simon, "Robust Regressor-Free Control of Rigid Robots Using Function Approximations," *IEEE Transactions on Control Systems Technology*, vol. 28, no. 4, pp. 1433-1446, 2020, <https://doi.org/10.1109/TCST.2019.2914634>.
- [44] S. A. Saadat, M. M. Fateh and J. Keighobadi, "Backstepping-based Adaptive Constrained Control of Passive Torque Simulator Using Function Approximation Technique," *International Conference on Electrical Engineering (ICEE)*, pp. 603-608, 2022, <https://doi.org/10.1109/ICEE55646.2022.9827263>.
- [45] L. Han, H. Wang, Z. Liu, W. Chen and X. Zhang, "Visual Tracking Control of Deformable Objects With a FAT-Based Controller," *IEEE Transactions on Industrial Electronics*, vol. 69, no. 2, pp. 1673-1681, 2022, <https://doi.org/10.1109/TIE.2021.3062277>.
- [46] N. D. Phu, V. V. Putov and C. T. Su, "Simplified Function Approximation Technique in Synthesis of Adaptive Control System for A Flexible Joint 4-DOF Robotic Manipulator with Executive Electric Drives," *International Conference on Control in Technical Systems (CTS)*, pp. 290-294, 2019, <https://doi.org/10.1109/CTS48763.2019.8973330>.
- [47] M. Abdelhady and D. Simon, "Prosthesis Controller-Hardware-in-the Loop Simulation," *3rd International Conference on Control and Robots (ICCR)*, pp. 134-139, 2020, <https://doi.org/10.1109/ICCR51572.2020.9344440>.
- [48] A. C. Huang and C. T. Huang, "FAT-Based Robot Adaptive Control with Position Measurements Only," *Chinese Control And Decision Conference (CCDC)*, pp. 3516-3520, 2019, <https://doi.org/10.1109/CCDC.2019.8833385>.
- [49] Y. Bai and M. Svinin, "Motion Planning and Control for a Class of Partially Differentially Flat Systems," *2th International Conference on Developments in eSystems Engineering (DeSE)*, pp. 855-860, 2019, <https://doi.org/10.1109/DeSE.2019.00158>.
- [50] S. Xu and B. He, "Adaptive Approximation Tracking Control of a Continuum Robot With Uncertainty Disturbances," *IEEE Transactions on Cybernetics*, vol. 54, no. 1, pp. 230-240, 2024, <https://doi.org/10.1109/TCYB.2022.3202540>.
- [51] H. F. N. Al-Shuka and E. N. Abbas, "Function Approximation Technique (FAT)-Based Nonlinear Control Strategies for Smart Thin Plates with Cubic Nonlinearities," *FME Transactions*, vol. 50, no. 1, pp. 168-180, 2022, <https://doi.org/10.5937/fme2201168A>.
- [52] S. M. A. Pahnehkolaei, J. Keighobadi, A. Alfi and H. Modares, "Compound FAT-Based Learning Control of Uncertain Fractional-Order Nonlinear Systems With Disturbance," *IEEE Control Systems Letters*, vol. 6, pp. 1519-1524, 2022, <https://doi.org/10.1109/LCSYS.2021.3119635>.
- [53] Y. Li, S. S. Ge, C. Yang, Xinyang Li and K. P. Tee, "Model-free impedance control for safe human-robot interaction," *2011 IEEE International Conference on Robotics and Automation*, pp. 6021-6026, 2011, <https://doi.org/10.1109/ICRA.2011.5979855>.